

Fault Displacement Hazards Analysis Workshop

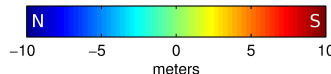
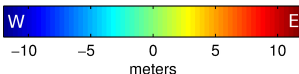
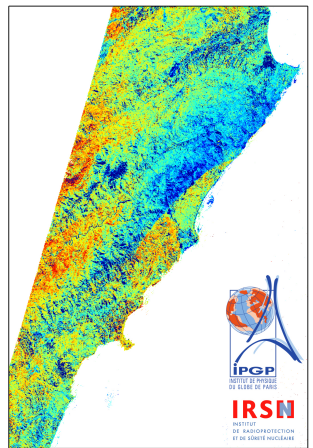
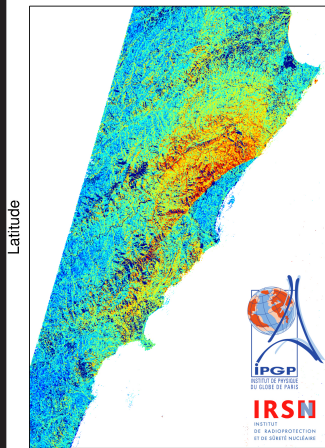
December 8 - 9, 2016

Menlo Park, CA



E-W Displacements (m)

N-S Displacements (m)





Fault Displacement Hazards Analysis Workshop Organizing Committee

Stéphane Baize

Institute for Radiological Protection and Nuclear Safety (IRSN)

Francesca Cinti

Istituto Nazionale di Geofisica e Vulcanologia (INGV)

Tim Dawson

California Geological Survey

David Schwartz

U.S. Geological Survey

The Organizing Committee would like to thank the following organizations for providing additional support for this workshop:



Lettis Consultants International (Coffee, pastries on December 8)

Pacific Gas and Electric (Lunch on December 8)

Earth Consultants International (Coffee, pastries on December 9)

Front Cover: Surface fault rupture, new analysis techniques, geologic characterization, and engineered mitigation are some of the themes of this Workshop. The 2016 earthquakes in Japan, Italy, and New Zealand provide a timely backdrop to this Workshop. *Top center:* 24 August, 2016 Monte Vettore fault rupture, Italy (Image provided by INGV). *Center left:* House damaged by surface rupture on the Kekerengu fault, New Zealand (Image from GNS Science). *Center right:* Fault rupture, Oh-Kirihata Dam, 2016 Kumamoto earthquake, Japan (Image from GEER 2016 report: Geotechnical Aspects of the 2016 M_w 6.2, M_w 6.0, and M_w 7.0 Kumamoto Earthquakes). *Lower left:* Sentinel 2A Micmac correlation maps of the 2016 Kaikoura Earthquake illustrating the use of remote sensing to quantify the deformation field due to surface rupture (Image by Johann Champenois (IPGP/IRSN)). *Lower right:* The Trans-Alaska Pipeline following the 03 November 2002 Denali Fault earthquake. The TAP Denali fault crossing remains one of the best examples of successful geologic fault characterization and engineering to mitigate the effects of surface fault rupture. (Photo credit: Tim Dawson).



Fault Displacement Hazard Analysis Workshop

December 8 – 9, 2016

Menlo Park, CA

December 8, 2016

Rambo Auditorium, Building 3

USGS Campus – 345 Middlefield Rd, Menlo Park, CA

8:00 – 9:00 Workshop Registration
9:00 – 9:30 Welcome and Introductory Remarks
(Dawson, Baize, Cinti, Schwartz)

Session I: Lessons learned from recent earthquakes

9:30 – 10:30

Surface rupture in the 2016 Earthquake Sequence in Central Italy
Francesca Cinti (INGV)

Widespread complex surface rupture associated with the Mw 7.0 16 April 2016 Kumamoto, Japan, earthquake
Shinji Toda (IRIDes - Tohoku University)

10:30 – 10:45 *Break*

10:45 – 11:45 Variation in earthquake surface rupture characteristics across intraplate Australia
Dan Clark (Geoscience Australia)

Fault rupture observations from the most recent and prior events along
New Zealand's Alpine Fault and Greendale Fault

Greg dePascal (University of Chile)

Constraining Co- and Post-Seismic Shallow Fault Slip with Near-Field
Geodesy and Mechanical Modeling

Ben Brooks (USGS)

11:45 – 12:00 Discussion of Issues Raised

12:00 – 13:30 *Lunch and collaborative informal discussions*

**Session II: Observational data for the Surface Rupture during Earthquakes (SURE)
Database**

13:30 – 15:00

Introduction to Session II – Perspectives from California

Tim Dawson (California Geological Survey)

Issues associated with setback distance from active fault in China: What
we have learned from the 2008 Wenchuan Earthquake

Xiwei Xu (China Earthquake Administration)

Quantifying Co-seismic Distributed Deformation Using Optical Image
Correlation: Implications for Empirical Earthquake Scaling Laws and
Safeguarding the Built Environment

Chris Milliner (U.C. Berkeley)

A new technique to measure 3D slip vectors from high-resolution
topography, applied to photogrammetry of historic ruptures

Austin Elliot (COMET/ University of Oxford)

Discussion

15:00 – 15:15 Break

**Session II: Observational data for the Surface Rupture during Earthquakes (SURE)
Database (Continued)**

15:15 – 16:15 50 or 500? Current Issues in Estimating Fault Rupture Length

David Schwartz (USGS)

Towards a unified database of Surface Ruptures (SURE): Objectives and perspectives

Stéphane Baize / Johann Champenois (IRSN)

16:15 – 17:00 Discussion

17:00 – 18:00 **Last minute addition:** Briefing on the 2016 Kaikoura, New Zealand Earthquake

Pilar Villamor (GNS Science)

18:00 Adjourn

(See next page for Day 2)

Fault Displacement Hazard Analysis Workshop Day 2

December 9, 2016

Menlo Park City Council Chambers

701 Laurel St. Menlo Park, CA

8:30 – 9:00 Workshop Registration
9:00 – 9:15 Overview/Observations from Day 1

Session III: Application and Advances in Deterministic and Probabilistic Fault Displacement Hazard Analysis

9:15 – 10:35

Fault displacement hazard at natural gas storage fields-a future research and regulatory direction

Thom Davis

U.S. criteria for assessing tectonic surface fault rupture and deformation at nuclear facilities

Ivan Wong (Lettis Consultants International)

Surface Rupture Data and Location Uncertainty in Probabilistic Fault Displacement Hazard Analyses

Mark Petersen (USGS) and Rui Chen (CGS)

Deterministic and probabilistic fault displacement hazard methodologies for gas pipeline crossings in California: applications and data needs

Steve Thompson (Lettis Consultants International)

10:35 – 10:50 *Break*

Session III: Application and Advances in Deterministic and Probabilistic Fault Displacement Hazard Analysis (Continued)

10:50 – 11:30

Risk Characterization and Dam Safety Modifications to Address Active Fault Rupture Beneath an Embankment Dam

Keith Kelson (U.S. Army Corps of Engineers)

Framework of probabilistic and deterministic methods for evaluating near-fault displacement

Naoto Inoue (Geo-Research Institute – Japan)

11:30 – 12:00

“Flash Talks”

Attendees are asked to present their top lessons learned in the applications of FDHA and the most pressing user needs in 1-2 slides, in about 2 minutes each. Sign-up sheet will be available at the Workshop (limited slots, first-come, first served!).

12:00 – 13:30

Lunch (On your own, see list of local restaurants and lunch options)

13:30 – 15:00

Application or Mis-Application of PFDHA. What Relationships are Appropriate and Is the Displacement Result Reasonable?

Donald Wells (Amec – Foster Wheeler)

Performance-Based PFDHA Using the Third Uniform California Earthquake Rupture Forecast

Glenn Biasi (University of Nevada, Reno)

Case Study of the Analysis and Design of Bridge Foundations Intersected by Active Faulting

James Gingery (Kleinfelder)

Engineering Implementation of the Results of a Fault Displacement Hazards Analysis

Jonathan Bray (U.C. Berkeley)

Discussion

15:00 – 15:15 *Break*

Session IV: Moving Forward

15:15 – 16:15

The Path Forward: Research Directions and Plans for a PEER Research Project

Norm Abrahamson (Pacific Gas and Electric)

Collaborative Opportunities and Coordination of Research Efforts

Jeff Bachhuber (PG&E), Yousef Bozorgnia (PEER)

16:15 – 17:00 Workshop Discussion and Wrap-up

17:00 *Adjourn*

Fault Displacement Hazards Workshop

December 8 – 9, 2016

List of Attendees

<u>First name</u>	<u>Last name</u>	<u>Affiliation</u>	<u>email</u>
Esam	Abraham	Southern California Edison	Esam.Abraham@sce.com
Norm	Abrahamson	Pacific Gas and Electric	NAA2@pge.com
Hans	AbramsonWard	Lettis Consultants International	abramsonward@lettisci.com
Eleanor	Ainscoe	Oxford	eleanor.ainscoe@earth.ox.ac.uk
Bob	Anderson	Seismic Safety Commission	anderson@stateseismic.com
Michael	Angell	Neogeologic	angell@neogeologic.com
Takashi	Azuma	Geological Survey of Japan	t-azuma@aist.go.jp
Jeff	Bachhuber	Pacific Gas and Electric	jxbs@pge.com
Stéphane	Baize	Institute for Radiological Protection and Nuclear Safety (IRSN)	stephane.baize@irsn.fr
Rob	Barry	CA Dept. of Water Resources	Rob.Barry@water.ca.gov
Glenn	Biasi	University of Nevada - Reno	glenn@seismo.unr.edu
Yousef	Bozorgnia	U.C. Berkeley - PEER	yousef@berkeley.edu
Jonathan	Bray	U.C. Berkeley	bray@ce.berkeley.edu
Ben	Brooks	U.S. Geological Survey	bbrooks@usgs.gov
Danny	Brothers	U.S. Geological Survey	dbrothers@usgs.gov
Bob	Budnitz	Lawrence Berkeley National Lab	budnitz@pacbell.net
Mike	Buga	Fugro	m.buga@fugro.com
Chung-Han	Chan	Earth Observatory of Singapore	chchan@ntu.edu.sg
Rui	Chen	California Geological Survey	Rui.Chen@conservation.ca.gov
Brian	Chiou	Caltrans	brian.chiou@dot.ca.gov
Francesca	Cinti	INGV	francesca.cinti@ingv.it
Dan	Clark	Geoscience Australia	Dan.Clark@ga.gov.au
Logan	Cline	Rizzo Associates	MLogan.Cline@rizzoassoc.com
Mike	Cline	Rizzo Associates	kmcgeo@gmail.com
Lloyd	Cluff	Consultant	lloydcluff@gmail.com
Kevin	Coppersmith	Coppersmith Consulting	kevin@coppersmithconsulting.com
Ryan	Coppersmith	Coppersmith Consulting	ryan@coppersmithconsulting.com
Thom	Davis	Geologic Maps Foundation, Inc.	davnamthom@aol.com
Tim	Dawson	California Geological Survey	Timothy.Dawson@conservation.ca.gov
Steve	DeLong	U.S. Geological Survey	sdelong@usgs.gov
Gregory	DePascale	University of Chile	gdepascale@ing.uchile.cl
Sadek	Derrega	Kleinfelder	SDerrega@kleinfelder.com

Mark	Dober	AECOM	mark.dober@aecom.com
Sean	Dunbar	CA Dept of Water Resources	Sean.Dunbar@water.ca.gov
Osman	El Menchawi	Fugro	oelmenchawi@fugro.com
Austin	Elliott	NERC-COMET	austin.elliott@earth.ox.ac.uk
Richard	Escandon	Kleinfelder	REscandon@kleinfelder.com
Reid	Fisher	Cal Engineering and Geology	rfisher@caleng.com
Yoshi	Fukushima	IAEA	Y.Fukushima@iaea.org
Eldon	Gath	Earth Consultants International	gath@earthconsultants.com
James	Gingery	Kleinfelder	JGingery@kleinfelder.com
Antonio	Godoy	James J. Johnson & Associates	agodoy@aon.at
Josh	Goodman	Fugro	j.goodman@fugro.com
Christine	Goulet	Southern California Earthquake Center	cgoulet@usc.edu
Tom	Hanks	U.S. Geological Survey	thanks@usgs.gov
Kathryn	Hanson	Consultant	Kathryn@klhansonconsult.com
Hoss	Hayati	SC Solutions	HHayati@scsolutions.com
Suzanne	Hecker	U.S. Geological Survey	shecker@usgs.gov
Chris	Hitchcock	Infraterra	chitchcock@infraterra.com
Jeff	Hoeft	Fugro	j.hoeft@fugro.com
Alan	Hull	Golder Associates	Alan_Hull@golder.com
Naoto	Inoue	Geo-Research Institute	naoto@geor.or.jp
Vince	Jacob	SC Solutions	vince@scsolutions.com
James	Johnson	James J. Johnson and Associates	jasjoh@aol.com
Annie	Kammerer	Consultant	annie@anniekammerer.com
Keith	Kelson	U.S. Army Corps of Engineers	Keith.i.kelson@usace.army.mil
Keith	Knudsen	U.S. Geological Survey	kknudsen@usgs.gov
Rich	Koehler	University of Nevada - Reno	rkoehler@unr.edu
Tyler	Ladinsky	Sage Engineers	tladinsky@sageengineers.com
Gregorios	Lavrentiadis	U.C. Berkeley	GLavrentiadis@fugro.com
Maryline	Le Beon	National Central University - Taiwan	mlebeon@gmail.com
Jongwon	Lee	Arup	jongwon.lee@arup.com
Bill	Lettis	Lettis Consultants International	lettis@lettisci.com
Nora	Lewandowski	Lettis Consultants International	lewandowski@lettisci.com
Zachary	Lifton	GeoSyntec	ZLifton@Geosyntec.com
Scott	Lindvall	Lettis Consultants International	lindvall@lettisci.com
Andy	Lutz	DWR - Division of Safety of Dams	Andrew.Lutz@water.ca.gov
Chris	Madugo	Pacific Gas and Electric	C7M0@pge.com
Marina	Mascorro	Langan Treadwell Rollo	mmascorro@Langan.com
Yasuhiro	Matsumoto	KOZO KEIKAKU Engineering	yasuhiro@kke.co.jp
Bill	McCormick	Kleinfelder	bmccormick@kleinfelder.com
Tim	McCrink	California Geological Survey	Tim.McCrink@conservation.ca.gov
Chris	Milliner	U.C. Berkeley	milliner@berkeley.edu

Mark	Molinari	AECOM	mark.molinari@aecom.com
Robb	Moss	Cal Poly - San Luis Obispo	rmoss@calpoly.edu
Josie	Nevitt	U.S. Geological Survey	jnevitt@usgs.gov
Koji	Okumura	Hiroshima University	kojiok@hiroshima-u.ac.jp
Nick	Oettle	AECOM	Nicolas.Oettle@aecom.com
Hector	Perea	U.C. San Diego	hperea@ucsd.edu
Mark	Petersen	U.S. Geological Survey	mpetersen@usgs.gov
Belle	Philibosian	U.S. Geological Survey	bphilibosian@usgs.gov
Joanna	Redwine	U.S. Bureau of Reclamation	jredwine@usbr.gov
Tom	Rockwell	San Diego State University	trockwell@mail.sdsu.edu
Alex	Sarmiento	GeoPentec	alexandra_sarmiento@geopentech.com
Kate	Scharer	U.S. Geological Survey	kscharer@usgs.gov
David	Schwartz	U.S. Geological Survey	dschwartz@usgs.gov
Oona	Scotti	Institute for Radiological Protection and Nuclear Safety (IRSN)	oonascotti@irsn.fr
Dogan	Seber	U.S. Nuclear Regulatory Commission	Dogan.Seber@nrc.gov
Anoosh	Shamsabadi	CA High Speed Rail Project	Anoosh.Shamsabadi@hsr.ca.gov
Xuhua	Shi	Earth Observatory of Singapore	xshi@ntu.edu.sg
Anna	Sojourner	CalTrans	anna.sojourner@dot.ca.gov
Janet	Sowers	Fugro	j.sowers@fugro.com
Alice	Stieve	U.S. Nuclear Regulatory Commission	Alice.stieve@nrc.gov
Ashley	Streig	Portland State University	streig@pdx.edu
Katsunori	Sugaya	Nuclear Regulation Authority, Japan	katsunori_sugaya@nsr.go.jp
Makoto	Takao	TEPCO	takao.makoto@tepcoco.jp
Robert	Tepel	Consultant	retgeo1@hotmail.com
Stephen	Testa	Testa Environmental Corporation	stesta@goldrush.com
Hong Kie	Thio	AECOM	hong.kie.thio@aecom.com
Patricia	Thomas	Lettis Consultants International	thomas@lettisci.com
Steve	Thompson	Lettis Consultants International	thompson@lettisci.com
Shinji	Toda	Tohoku University - Japan	toda@irides.tohoku.ac.jp
Masao	Tonagi	KOZO KEIKAKU Engineering	tonagi@kke.co.jp
Gabriel	Toro	Lettis Consultants International	toro@lettisci.com
Pilar	Villamor	GNS Science (Te Pū Ao)	P.Villamor@gns.cri.nz
Melanie	Walling	AECOM	melanie.walling@aecom.com
Yu	Wang	Earth Observatory of Singapore	Y.Wang@ntu.edu.sg
Janet	Watt	U.S. Geological Survey	jwatt@usgs.gov
Donald	Wells	AMEC-Foster Wheeler	Donald.wells@amec.com
Ivan	Wong	Lettis Consultants International	wong@lettisci.com
Katie	Wooddell	Pacific Gas and Electric	katie.wooddell@gmail.com

Xu	Xiwei	Institute of Geology, China Earthquake Administration	xiweixu@vip.sina.com
Bob	Youngs	AMEC-Foster Wheeler	bob.youngs@amecfw.com
Zia	Zafir	Kleinfelder	ZZafir@kleinfelder.com

Towards a unified and worldwide database of surface ruptures (SURE)

S. Baize, J. Champenois, F. Cinti, T. Dawson, A. Elliott, L. Guerrieri, Y. Klinger, J. McCalpin, K. Okumura, O. Scotti, M. Takao, P. Villamor, R. Walker

Assessing Fault Displacement Hazard is based on empirical relationships that are derived from regressions of earthquake data. The regressions that are used so far are based on sparsely populated datasets, mainly including a restricted number of pre-2000 events. A common effort has started in 2015 to constitute a worldwide, unified and shared database to improve further estimations, with the support of INQUA. The SURE database would update published databases that relate earthquake magnitude to surface faulting (both primary and distributed faulting). In October 2015, IRSN sponsored a workshop during which earthquake geologists started discussions for building such a database. The group observed that the existing datasets hold very limited description and parametrization of the rupture, only including magnitude and kinematics of event, coordinates and net slip of the measured points (e.g., Pezzopane and Dawson, 1996; Petersen et al., 2011; Takao et al., 2013). We emphasized that future cases could be implemented with more details.

How to improve the description of surface ruptures?

Recent events highlighted that the modern techniques, such as SAR interferometry, LiDAR or SfM topography, allow the recognition of an extensive picture of coseismic deformation. The geologist work was facilitated by the InSAR maps available in the early phase after the 2014 M6 Napa earthquake (DeLong et al., 2016). The M5 26/3/2010 Pisayambo, Ecuador, earthquake rupture would not have ever been recognized without InSAR, in this remote and high-elevation region of the Andes (Champenois et al., submitted). LiDAR imaging can provide accurate estimation of offsets, potentially providing a huge amount of data to appreciate the natural variability of surface faulting and to quantify uncertainties (Gold et al., 2013). Probably the improvement of detection capacity with modern techniques would erase the difference of surface rupture probability between Japan and western USA reported by Takao et al. (2013): these two active countries have very different morpho-climatic contexts that could largely have influenced detection of historical cases' surface rupture with classical mapping. Indeed, evidencing M5-6 earthquakes surface rupture with classic field mapping is easier in southern California (e.g. Suarez-Vidal et al., 2007) than under the Japanese canopy. The recent M7 Kumamoto earthquake nicely illustrates this: subtle deformation evidences under the Aso caldera flank canopy were highlighted thanks to SAR (Fujiwara et al., 2016).

With InSAR development, we underline that a comprehensive overview of the earthquake-related deformation is now available at the source scale, even for big quakes ($M > 7$). In the crustal slab that has been strained during the interseismic period, released elastic deformation during earthquake can be distributed in this zone (strain rebound). Typically, this zone can be larger than 15 km on the hanging wall during M7+ normal earthquakes and similar volumes might be considered for strike-slip events. Therefore, the convention to consider as "triggered" each rupture beyond 2 km (Petersen et al., 2011) might be revised. An idea to explore could be considering slip as triggered when occurring beyond the geodetic deformation field. One issue we have to figure out is: would the database include triggered slip measurements as it was in the existing normal fault database (Youngs et al., 2003)? In the specific case of normal faults, we note that there is potentially the risk to handle "misleading" values including a gravitational component. In the examples of normal faults in the Italian Apennines, several historical cases (including the last ones in 2016) have been the subject of such controversy. How to handle this potential bias, if any? In the proposed database structure, we included a "slope" parameter that could be used as a flag to generate specific regressions.

Japanese and US practitioners have different approaches to determine the “primary” vs “distributed” character. In Japan, once the main rupture is identified from geological and seismological data, the “distributed” character is assigned to any slip clue beyond a pre-defined distance off this main trace. This threshold is determined as the 1%-main-trace-length width. On the contrary, the US approach is empirical, essentially based on evaluation of structural relationships between ruptured segments. Whatever the technique, some complex cases such as the M7.2 2010 El Mayor-Cucapah rupture would require an elaborated structural model to rank the segments and define the main rupture (e.g. Fletcher et al., 2016). Another issue that we have to cope with is the calculation of distances from distributed clues to primary fault plane. In cases with partly buried main rupture with distributed faulting at the surface (e.g. Edgecumbe, New Zealand, 1987), we have to select a strategy: whether to use the rough earthquake fault plane determined from seismological data or calculate distance to the nearest primary surface traces. For blind primary ruptures, we might calculate distance to the intersection between ground surface and fault projection, or measure distance to the fault plane (see GMPEs metrics such as R_{jb} , R_x and R_{rup}).

Recent earthquake cases like El Mayor-Cucapah (2010, Mexico) (Teran et al., 2015) or sand-box models (Stanton, 2013) have shown that surface geology control the rupture pattern. In the Mexican example, both the number of slip planes and their geometry are influenced by the nature of affected rocks. In the experimental results, the near-surface material stiffness is another crucial parameter influencing the rupture pattern and fabric. Recently, Moss et al. (2013) confirmed, based on an extensive dataset of surface ruptures and V_{s30} , that the stiffness of surface deposits has a strong impact on the propagation of rupture to the ground surface for reverse faults, but not for strike-slip faults. They also conclude that V_{s30} is useful in predicting the width of deformation band above the primary fault: stiff deposits will have a “brittle” response and a narrow fault zone, whereas ductile behavior or distributed deformation will occur in regions with loose sediments.

During discussions at the Paris meeting, the structural pattern of master fault was also promoted as a potential control parameter. It appears that distributed faulting does not have a uniform density along strike and is much more common at step-overs, bends, and other geometric irregularities (e.g. 2013 M7.7 Balochistan event; Vallage et al., 2013). To account for this, we propose to empirically discretize fault portions along the strike of historic surface ruptures into simple or complex, and then make separate regressions. As soon as the late '80s, Bonilla (1988) also introduced that fault geometry at depth could largely control surface faulting: for instance, the large to very large crustal earthquakes that hit Argentina in 1944 (M7 & 7.5, La Laja) did not produce primary surface rupture because the fault plane was gently dipping, so that the rupture could not reach the surface despite large M. In addition, the focal depth vs shear modulus, which have never been considered in scaling laws or rupture probability regressions, are crucial parameters that may need to be considered (Bonilla, 1988).

Potential structure of the future SURE database

The unified database to be implemented is mainly dedicated to future probabilistic studies, and will include primary and distributed faulting information. To upgrade existing databases, it will incorporate new parameters to describe surface rupture data such as surface geology, focal depth, and structural pattern or fault complexity. During the October 2015 meeting in Paris, the attendees agreed on a preliminary list of fields to fill in, split into three spreadsheets. The “earthquake sheet” describes all the parameters associated with the earthquake source (magnitude, depth, seismological parameters such as rupture length at depth, fault width, geodetical information). A “fault portion sheet” compiles the mapping information of surface rupture segmentation, structural complexity and segment history (paleoearthquakes, slip rate

etc, when available). The crucial information in the “observation point table” is the measured net slip, and the primary or distributed class assignment.

In the Paris meeting follow-up phase, the contributors provided datasets of historical cases including 1944 M7.0 and M7.4 La Laja (Argentina), 1959 M7.0 Hebgen Lake (USA), 1983 M6.9 Borah Peak (USA), 1987 M6.3 Edgecumbe (New Zealand), 1995 M6.9 Kobe (Japan), 2009 M6.3 L’Aquila (Italy) earthquakes. M. Takao also provided the complete data on 19 historical events that constitute the Japanese dataset used in PFDH analyses in Japan, covering the 5.8 to 7.4 (Takao et al., 2013). We could also easily include the 2002 M7.9 Denali (Alaska, USA) and 2010 M7.2 El Mayor-Cucapah (Mexico) earthquakes’ datasets which are online. Excluding the last event, the coseismic displacement descriptions are lacking in surface geology, structural complexity and other parameters discussed in Paris. Another step when creating the SURE database will have to consider all the post-2000 inland earthquakes down to M=6.0, which potentially could provide relevant data after investigation with accurate techniques; this will enable including as much as possible various tectonic contexts. McCalpin (2006) performed this first search in the USGS earthquake database (<http://earthquake.usgs.gov/earthquakes/search/>), thus compiling a catalog of 130 shallow M6+ epicenters onshore between 2000 and 2016. Most occurred in China (21), Iran (13), Japan (8), Russia (8), Pakistan (7), Turkey (7), New Zealand (6), Kyrgyzstan (5), USA (5), Chile (5), Nepal (5), Myanmar (4). Very few have surface rupture information reported in literature and there is a need for regional geologists’ participation. This will be one major task of the SURE working group in the next years.

Conclusion

The Menlo Park meeting is a unique opportunity to discuss the relevance of such a database structure. The feedback of GMPEs has to be accounted for: the seismological community introduced, through the accumulation of data during the last years, many parameters to constrain the regressions. The number of these regressions increased exponentially and it became a plain exercise to select the appropriate GMPEs in PSHA.

Implementing such a database will be time-consuming and will require sponsorship: Who? Where? How? The database must be free and downloadable, because data will be freely and voluntarily provided and shared at the worldwide scale. An appropriate platform for this will also have to be set up. The final aim is to provide flat-files with homogeneously computed quantities that can then be used to derive different displacement regression equations.

References

Bonilla M. (1988). Minimum Earthquake Magnitude Associated with Coseismic Surface Faulting. Bulletin of the Association of Engineering Geologists, Vol. XXV, No. 1, pp. 17-29.

Champenois J. et al. Evidences of surface rupture associated with a low magnitude (M5.0) shallow earthquake in the Ecuadorian Andes. Journal Geophysical Research, submitted.

DeLong S. B. et al. (2016). Tearing the terroir: Details and implications of surface rupture and deformation from the 24 August 2014 M6.0 South Napa earthquake, California. Earth and Space Science, 3, doi:10.1002/2016EA000176.

Fletcher J. et al. (2016). The role of a keystone fault in triggering the complex El Mayor–Cucapah earthquake rupture. Nature Geoscience, DOI: 10.1038/NGEO2660.

- Fujiwara et al. (2016). Small-displacement linear surface ruptures of the 2016 Kumamoto earthquake sequence detected by ALOS-2 SAR interferometry. *Earth, Planets and Space*, 68:160, DOI 10.1186/s40623-016-0534-x.
- Gold R. et al. (2013). Coseismic slip variation assessed from terrestrial lidar scans of the El Mayor–Cucapah surface rupture. *Earth and Planetary Science Letters*, 366, 151–162.
- McCalpin J. (2016). List Of Recent Earthquakes That Possibly Had Surface Rupture [Data set]. Zenodo, <http://doi.org/10.5281/zenodo.154767>.
- Moss R. et al. (2013). The Impact of Material Stiffness on the Likelihood of Fault Rupture Propagating to the Ground Surface. *Seismological Research Letters*, May/June 2013, v. 84, p. 485-488.
- Petersen M. et al (2011). Fault Displacement Hazard for Strike-Slip Faults. *Bulletin of the Seismological Society of America*, Vol. 101, No. 2, pp. 805–825, doi: 10.1785/0120100035.
- Pezzopane S. and Dawson T. (1996). Fault displacement hazard: a summary of issues and information. In *Seismotectonic Framework and Characterization of Faulting at Yucca Mountain*, Whitney, J. W. (Editor), Department of Energy, Las Vegas, 9-1 – 9-160.
- Stanton K. V. (2013). Investigation of parameters influencing reverse fault rupture propagation to the ground surface. Thesis “Master of Science in Civil and Environmental Engineering”, Faculty of California Polytechnic State University, San Luis Obispo.
- Suarez-Vidal F. et al. (2007). Surface Rupture of the Morelia Fault Near the Cerro Prieto Geothermal Field, Mexicali, Baja California, Mexico, during the Mw 5.4 Earthquake of 24 May 2006. *Seismological Research Letters* Volume 78, Number 3.
- Takao M. et al., (2013). Application of Probabilistic Fault Displacement Hazard Analysis in Japan. *Japan Association for Earthquake Engineering* 13, 1.
- Teran O. et al., 2015. Geologic and structural controls on rupture zone fabric: A field based study of the 2010 Mw 7.2 El Mayor–Cucapah earthquake surface rupture. *GEOSPHERE*; v. 11, no. 3, doi:10.1130/GES01078.1.
- Vallage A. et al. (2013). Inelastic surface deformation during the 2013 Mw 7.7 Balochistan, Pakistan, earthquake. *Geology*, doi:10.1130/G37290.1.
- Youngs R. R. et al., (2003). A Methodology for Probabilistic Fault Displacement Hazard Analysis (PFDHA). *Earthquake Spectra*, 19, 1, 191–219.

Performance-Based PFDHA Using the Third Uniform California Earthquake Rupture Forecast

Glenn Biasi
University of Nevada Reno
Seismological Laboratory, MS 174
Reno, NV 89557
glenn@unr.edu

Introduction

Seismic resilience for California depends heavily on being able to maintain lifeline levels of utility services following a large earthquake. Water and gas supplies in particular are exposed to hazards of physical ground rupture during earthquakes. In southern California (SoCal) aqueducts including the California Aqueduct from northern California, the Los Angeles Aqueduct from the eastern Sierras, and the Colorado River Aqueduct constitute the main water sources. All three cross multiple active faults of southern California, and could be damaged simultaneously in a major San Andreas fault (SAF) event.

Risks from ground rupture might in principle be just a matter of engineering, but in practice resources are limited, and engineers and managers rely on risk-benefit assessments to mitigate risks and schedule system improvements. A performance-based engineering approach to resilience requires geologic hazards and uncertainties to be cast in probabilistic terms. The full estimation of risk to pipeline, aqueduct and other utility assets requires a systems approach and a multidisciplinary team including geologists, seismologists, and engineers. This paper addresses how the Uniform California Earthquake Rupture Forecast 3 (UCERF3) can be used to quantify on-fault surface displacement offsets on the main active faults in California. The process is readily applied to strike-slip fault crossings anywhere in the UCERF3 fault model.

Performance-based fault displacement estimation using UCERF3

The current state of practice for seismic hazard in California is defined by the Uniform California Earthquake Rupture Forecast 3 (Field et al., 2014). This project resulted in ground rupture rates for active faults of California where a slip rate was available as a constraint. UCERF3 models the fault system using ~2600 “subsections”, discrete fault panels of ~7.5 km in strike length that extend to the base of the seismogenic layer. Slip within a subsection is modeled as constant. Earthquakes on this system rupture two or more adjacent subsections. To cover “all possible ruptures”, all unique combinations of subsections were formed; this ran to 253,706 ruptures for the simpler Fault Model 3.1 (FM3.1), and over 300,000 for FM3.2. Annual rates of occurrence for these ruptures were developed using the Grand Inversion (GI; Page et al., 2014), with fault slip rates, paleoseismic event rates, and regional seismicity as most influential data constraints. For probabilistic fault displacement hazard analysis (PFDHA) at any specific fault crossing, the UCERF3 model provides most of the main ingredients: rupture locations and annual rates everywhere in the fault model. Thus the hazard at a fault crossing is estimated within UCERF3 by the total slip among ruptures using the subsection crossed. Each subsection has a unique identifying number within a fault model; we use those numbers as a shorthand reference device. We use UCERF3 FM3.1 and the branch-averaged mean solution to illustrate our approach.

We illustrate the basic procedure for using UCERF3 rupture rates with a project site (“CAA West”) where the California Aqueduct (CAA) crosses the San Andreas fault (SAF) near Fort Tejon (Figure 1). The UCERF3 solution uses 67,931 ruptures to model the earthquake hazard of the SAF to the site (Figure 2). Most of these ruptures are large ($7.6 < M < 8.35$), long, and end far from the project site.



Figure 1. California Aqueduct (black sinuous line through lake) crossing the SAF (orange line) near the map pin. This area is also a transportation corridor; Interstate 5 is visible on the left side. The SAF slips at 20-35 mm/yr here (UCERF3 rate = 26 mm/yr), and last slipped in 1857.

Figure 2. (right) Individual rupture annual rates (red stars) and summary magnitude-frequency distribution (blue line) for ruptures passing through Su1833, which includes CAAWest. Points in the summary MFD could be used for hybrid probabilistic/deterministic hazard applications with UCERF3 annual rates.

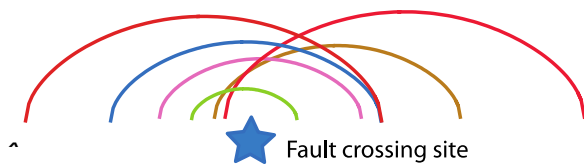
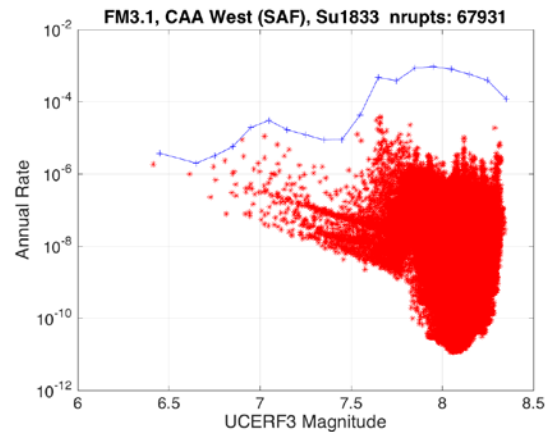


Figure 3. Rupture displacements in an earthquake have an approximate average shape (shown as elliptical arcs) around which they vary. The site (blue star) will be in the middle of some, and the tapering end of others. Vertical dimension is the displacement, which scales from AD. The peak in this shape is $1.31 \cdot AD$, much less than the variability of real ruptures. The analytic shape gives a base estimate for fault displacement.

Fault displacement depends on whether the project site is in the middle of a rupture, where displacements are generally above the event average displacement (AD), or near the end where displacements taper to zero (Figure 3). Rupture model average displacement can be found using an analytic shape, $D = AD \cdot \sqrt{\sin(\frac{\pi x}{L})}$, where x/L is the normalized site location in a rupture of length L (Biasi et al., 2013).

Variability of D around the mean shape also depends on fractional location x/L (Figure 4). Conceptually, we could use the mean and standard deviation at station x/L in Figure 4, but this could lead to unphysically large displacements. Instead we make histograms of the variability data itself in bins of x/L , and sample from those distributions. This limits upper tails of

displacement to D/AD values observed in real data. We also find that variability is more extreme among displacement profiles of small strike slip events than for large ones.

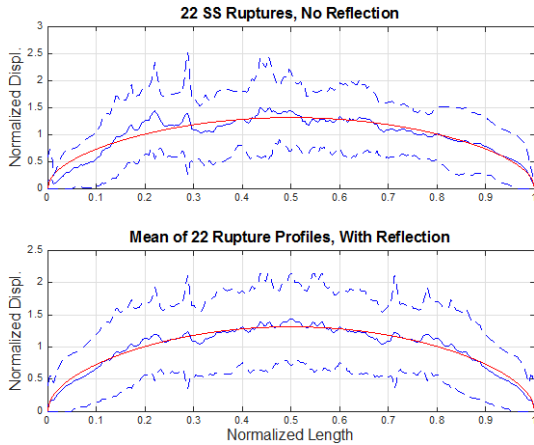


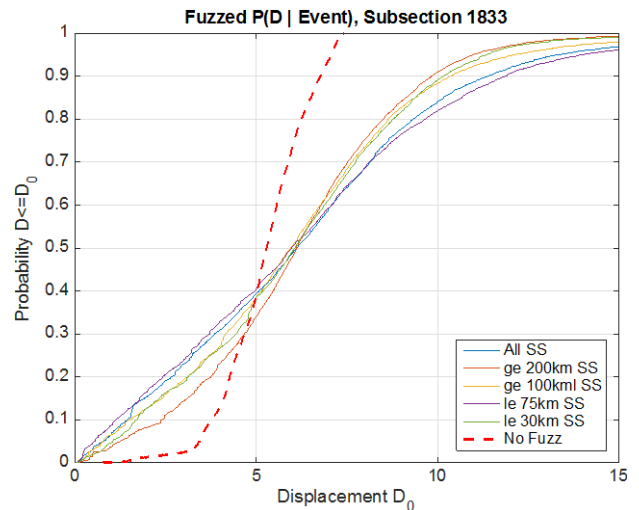
Figure 4. Unreflected and reflected normalized displacement profiles for 22 strike-slip surface ruptures (Biasi et al., 2013). Vertical axis is normalized displacement. The red line analytic shape is not fit to the data, only drawn over it. Dashed lines show 1-sigma variation around the mean. +1-sigma displacements of $2 \cdot AD$ are realistic in the central 50% of rupture extent based on actual rupture data.

The probability of each rupture is known from the UCERF3 solution, so probabilities and corresponding displacements can be tabulated and arranged as a cumulative distribution (CDF) of D vs. probability of exceedance (Figure 5). The heavy red dashed line shows displacement from the analytic shape only. If only the analytic shapes are used, displacement at the CAAWest site has only a 10% chance of being smaller than 3.7 m. When displacement variability is added, the displacement distributions flatten to increase weight among smaller displacements. The individual colored lines show that the displacement CDF depends on the set of strike-slip rupture profiles used to estimate variability (see legend). From this we concluded that best results would be to apply the variability subset most like the input rupture length (e.g., the “le 30 km SS” to a rupture shorter than 30 km). The CDF weighted in that way is close to the “ge 200km SS” set in **Figure 5** because most ruptures through the CAAWest site are much longer than 200 km. All subsets agree near the $D_{50} = 50\%$ likely displacement estimate of 6.2 m. This is not out of keeping with measurements from the 1857 rupture. Maximum displacements reach 2.5 to 3 AD. We will be pursuing research to limit extremes in rupture displacement variability.

Figure 5. Probability of displacement on the UCERF3 fault trace at CAAWest given that an earthquake ruptures there. Displacement axis has been limited to preserve overall plot scale. Dashed line has no displacement variability; other lines come from five subsets of the strike-slip (SS) data as indicated in the legend.

Annual rates and return times

Displacement probabilities conditioned on event occurrence (**Figure 5**) are useful for scenario planning, but actual annual rates of occurrence of the displacement are needed for benefit-risk estimation. Time-independent annual rates as a function of displacement can also be estimated from UCERF3 results (Figure 6). At the smallest displacements, the rate (or return time) represents the UCERF3 rate for any ground rupture. Return times are relatively similar up to ~6 m, with significantly decreased rates for large displacements. Still displacements of 8.4 m are expected with 1000 year return times.



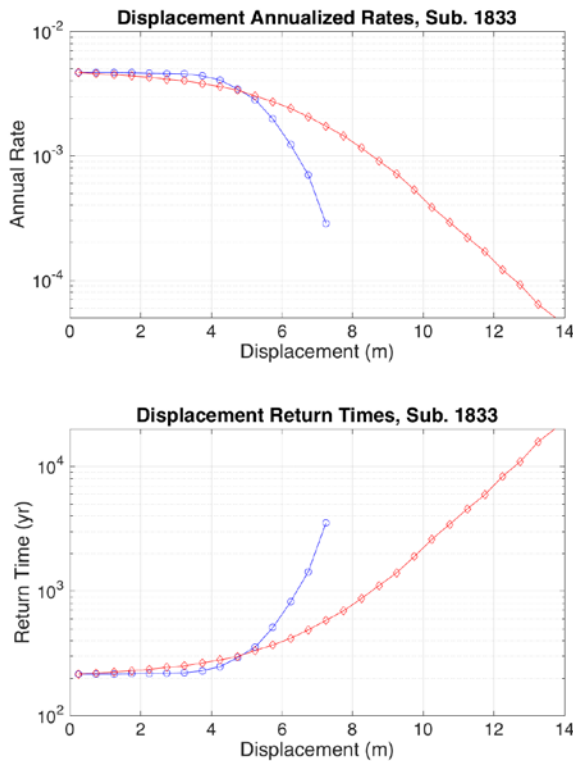


Figure 6. Absolute annual rates and return times of displacements at the CAAWest site. Blue line assumes the analytic rupture shape only. Red line includes length-consistent variability “fuzzing”. Displacements of 8.4 m are predicted about once per 1000 years at the site.

Development plans

Observations from repeated fault displacements at a point suggest a greater degree of consistency in displacements than from displacement profiles in general. Hecker et al. (2013) find a log sigma variability in point displacement of ~0.5 based on paleoseismic and geologic estimates. We plan to estimate the variability in the UCERF3 rupture set, and may find a basis for adjusting downward the weight given largest ruptures. Although out of scope for this work, future UCERF iterations may place less weight (i.e., compared to Figure 2) on long through ruptures.

Conclusions

UCERF3 defines the state of practice in terms of California earthquake forecasts, so going forward, the ability to use these results is likely to be of interest to utility owners and engineers. Well-posed probability distributions for on-fault surface rupture displacements can be formed directly from the UCERF3 results. These probability distributions comprise an essential input for performance-based engineering assessment for resilience applications. Because of the structure of UCERF3, these results are in one sense simpler than previous PFDHA practice, being obtained without resorting to scaling relations, floating ruptures, or other assumptions about rupture configuration on the fault. Although not shown here, epistemic uncertainty in fault slip rate is readily included. San Andreas fault crossings can expect large median displacement hazard estimates, in part because the SAF is southern California’s largest fault, and in part because of the relatively higher weighting on large earthquakes in UCERF3. The west California Aqueduct crossing conditional D_{50} estimate of 6.2 m could present a significant challenge for engineering mitigation. Future developments may point to ways to reduce some upper estimates of potential displacements.

References

- Biasi, G. P., R. J. Weldon II, and T. Dawson (2013). Distribution of slip in ruptures, U.S.G.S Open-File Report 2013-1165, Uniform California Earthquake Rupture Forecast Version 3 (UCERF3) – The Time-Independent Model, Appendix F, 41 pp.
- Field, E. H., R. J. Arrowsmith, G. P. Biasi, P. Bird, T. E. Dawson, K. R. Felzer, D. D. Jackson, K. M Johnson, T. H. Jordan, C. Madden, A. J. Michael, K. R. Milner, M. T. Page, T. Parsons, P. M Powers, B. E. Shaw, W. R. Thatcher, R. J. Weldon II, and Y. Zeng (2014) Uniform

- California Earthquake Rupture Forecast Version 3 (UCERF3) – The Time-Independent Model, *Bull. Seismol. Soc. Am.*, 104, 1122-1180.
- Hecker, S., N. A. Abrahamson, and K. E. Wooddell (2013). Variability of displacement at a point: Implications for earthquake-size distribution and rupture hazard on faults, *Bulletin of the Seismological Society of America*, 103, 651-674.
- Page, M. T., E. H. Field, K. R. Milner, and P. M. Powers (2014). The UCERF3 Grand Inversion: Solving for the long-term rate of ruptures in a fault system, *Bull. Seism. Soc. Am.*, 104, 1181-1204.

Engineering Implementation of the Results of a Fault Displacement Hazards Analysis

Jonathan D. Bray, Ph.D, P.E., NAE
University of California, Berkeley

Insights from field observations of surface fault rupture are discussed with special emphasis on describing how ground movements resulting from surface faulting affect structures. Recent experimental and analytical studies of the interaction of surface faulting with structures are presented. Findings from the field, experimental, and analytical studies identify effective design strategies which can be utilized to mitigate the hazards associated with surface faulting. These design measures include establishing non-arbitrary setbacks based on fault geometry, fault displacement, and the overlying soil; constructing earth fills, often reinforced with geosynthetics, to partially absorb underlying ground movements; using slip layers to decouple ground movements from foundation elements; modifying the ground to deflect the majority of the movement, and designing strong, ductile foundations that can accommodate some deformation without compromising the functionality of the structure.

Constraining Co- and Post-Seismic Shallow Fault Slip with Near-Field Geodesy and Mechanical Modeling

Ben Brooks

Josie Nevitt

USGS ESC, Menlo Park

The nature of earthquake-related fault slip in the shallowest portion of Earth's crust is still very poorly known. Without better quantification of shallow fault slip, we are likely limiting not only our understanding of fundamental fault-slip physics but also seismic hazard associated with near-surface rupture. If, for instance, near-surface vertical gradients in fault slip are non-negligible and it is assumed that surface observations of fault-parallel displacement are equivalent to slip across a fault at shallow depths, then slip rates used in probabilistic seismic hazard assessments could be underestimated. Similarly, the contribution of 'off-fault deformation' to a slip event (either co- or post-seismic) is critical in terms of accurately assessing shallow fault slip. However, studying shallow fault slip any deeper than the few meters typically exposed by trenches has been limited by sparse geodetic observations in the near-field (within ~1 km) of a fault's trace. Recently, a new generation of near-field geodetic imaging techniques is filling in the observational gap and providing unprecedented, spatially dense, near-field observations. Although these data permit strikingly detailed observations of near-field surface displacement fields, inferring shallow fault slip requires mechanical and dynamic models of the shallowest 100-200 meters of Earth's crust. Here, we discuss some of the practical aspects faced with analyzing the new wealth of near-field data. We discuss generally how different shallow material properties (cohesion, angle of internal friction, fault friction) are expected to affect near-field geodetic data as well as conceptualization of off-fault deformation. We report specifically on Mobile Laser Scanning studies of the principal surface disruption trace associated with the August 2014 M6 South Napa Earthquake. We use an elastic model to invert the surface displacements of deformed vineyard rows for a model that simultaneously constrains both slip and depth of slip. Combined with evidence from trenches, we find that despite its classification as a 'surface-rupturing' earthquake slip did not breach the surface but, rather, terminated at varying depths along strike from ~3 to as much as ~25 meters. Estimated slip values can be significantly greater than observed surface offset of vine rows (made by tape measure, for instance), especially where the fault tip is deepest. Finally, for buried faults, we show that previous metrics of 'off-fault deformation' do not accurately assess the amount of plastic and/or distributed brittle faulting associated with a specific fault: for the South Napa event, however, it appears there is minor off-fault deformation associated with the principal rupture.

Surface rupture in the 2016 Earthquake Sequence in Central Italy

Francesca R. Cinti*

Emergeo Working Group, Istituto Nazionale di Geofisica e Vulcanologia, Italy

Starting from 24 August 2016, a normal faulting earthquake sequence characterized by multiple mainshocks severely struck Central Italy. Following a Mw6.0 earthquake (Amatrice mainshock, 24th August), a Mw5.9 (Visso mainshock, 26th October) occurred about 25 km to the north, and after four days the sequence culminated with a Mw6.5 event (Castelluccio mainshock, 30th October) located in between the previous two. The three events nucleated within 8 km of depth and ruptured different portion of the same fault system, the Mt. Vettore-Mt. Bove fault system. Thousands of observations of different types of coseismic geological effects were recorded within a ~1000 km² wide area during the two months of intense seismicity. Among these several data of the coseismic ruptures along the faults of the sequence area have been collected by the Emergeo team also in collaboration with National and International Universities and Research Centers. Although the data survey and analysis are still ongoing, based on the ruptures characteristics, distribution and displacement amplitudes, we may infer that: - the Amatrice Mw6.0 event produced about 5 km long primary normal surface faulting with an average surface vertical displacement of 0.13 m along the southern portion of the Mt. Vettore-Bove fault system; - the Visso Mw5.9 event produced ruptures along different northern fault splays of the Mt. Vettore-Bove system, with vertical displacement locally in the range of 0.6-0.8 m. Data relative to this major event are incomplete being soon overprinted by the immediate Mw6.5 mainshock; - the Castelluccio Mw6.5 mainshock produced about 20 km of primary normal surface faulting along the Mt. Vettore-Bove system. The rupture run along fault splays, previously "locked", in the central portion of the system and partially overlapped with the Amatrice and Visso ruptures, increasing the amplitude of the displacement. The amount of offset measured on the eastern fault splay locally exceeds 2 m, however the general trend along the southwest-dipping faults is around 0.8 m. Also antithetic faults belonging to the fault system ruptured with vertical displacement exceeding the 0.5 m. The distribution analysis of the data is in progress.

The earthquake fault rupture has been structurally controlled by pre-existing lineaments inherited by the past compressional tectonics. These latter are responsible for the fault segmentation in the central Apennines. Then, we have a strong confirmation that a key to unravel the anatomy of the normal faults possibly responsible for magnitude earthquakes ranging between 5.5. and 7.0 in such environments requires detailed fault survey and paleoseismic data. Finally, the 2016 Central Italy earthquake sequence is a case of study that has been seldom observed so far and definitively provides new data and insights, also for supporting a worldwide surface faulting database (SURFACE - SURface FAulting Catalogue Earthquakes, INQUA project 2016-2019).

Variation in earthquake surface rupture characteristics across intraplate Australia

Dan Clark

dan.clark@ga.gov.au

Geoscience Australia, GPO Box 378 Canberra, ACT, 2601, Australia.

Geometries for over 350 Quaternary-active faults are captured in the Australian Neotectonic Features Database (Clark *et al.*, 2012) (Figure 1). Of these, eight relate to historic ruptures and only a handful have been the subject of palaeoseismological investigation to determine seismic source parameters such as earthquake magnitudes and recurrence characteristics. Despite this, variation in fault scarp length, vertical displacement, proximity to other faults and relationship to topography permits division of the continent according to seismogenic character/potential. Six onshore “neotectonic domains” are recognised, with an additional offshore domain proposed by analogy with the eastern United States. Each domain relates to a distinct underlying crustal type and architecture, broadly considered to represent cratonic (Precambrian), non-cratic (Phanerozoic accretional terranes) and extended (e.g. aulacogen, passive margin) environments (Figure 1). In general, greater topographic expression associated with faults occurring in extended crust relative to non-extended crust suggests a higher rate of seismic activity in the former setting, consistent with observations worldwide (e.g. Talwani, 2014). Using the same reasoning, non-cratic crust might be expected to have a higher seismogenic potential than cratonic crust. These observations are consistent with models relating seismogenic potential to lithospheric thickness (Mooney *et al.*, 2012).

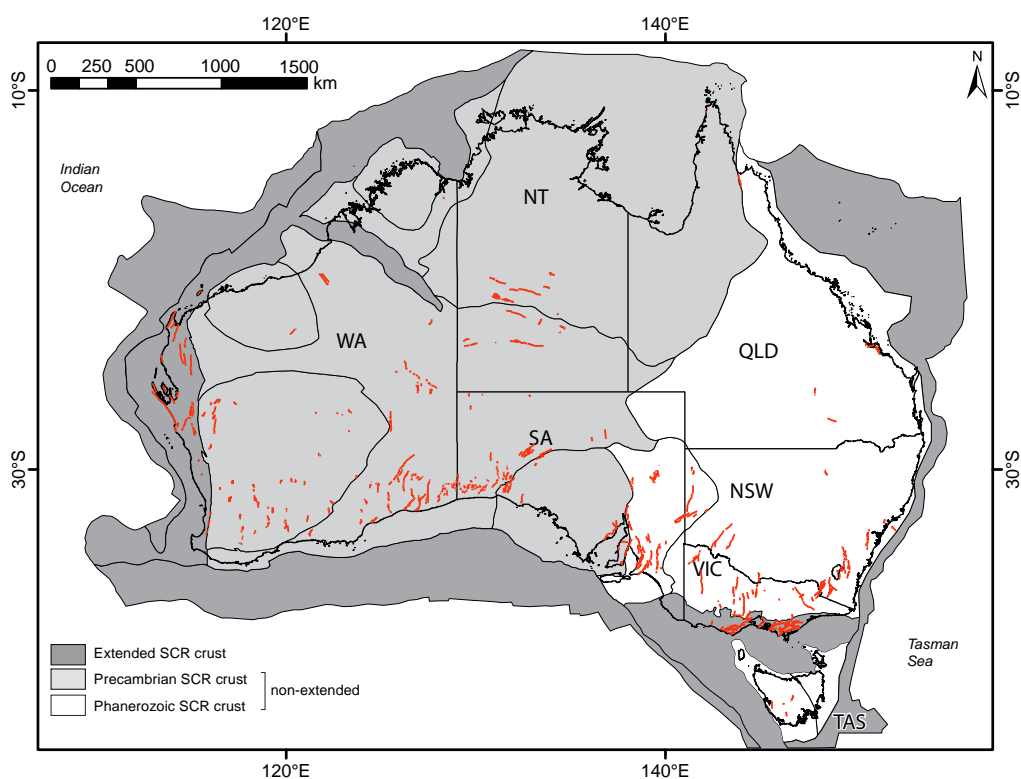


Figure 1: Neotectonic features from the Australian Neotectonic Features database (red lines) overlaid onto the neotectonic domains model of Clark *et al.* (2012), shaded to emphasise cratonic and non-cratic domains.

The variation in rupture characteristics directly influences how fault rupture hazard might be assessed. In the cratonic parts of the continent, ruptures are short (<50 km),

isolated, and often very complex in plan form (Figure 2a). Scarps are very modest in height (<10m in Archaean, <20 m in Proterozoic), indicating either that uplift rates commensurate to the very low erosion rates, or that strain localization on individual faults is transient. Evidence for a maximum of four events, and more commonly one to three events, has been observed from individual faults over Quaternary timescales (Clark *et al.*, 2008; Clark *et al.*, 2011; Crone *et al.*, 2003; Crone *et al.*, 1997; Estrada, 2009; Whitney *et al.*, 2015). All of the eight historic surface rupturing earthquake events (Table 1), including the May 21st Mw6.0 Petermann Ranges earthquake, occurred on faults that could not have been mapped using topographic signature prior to the event. The dominance of ‘one-off’ ruptures in unanticipated places is consistent with recently published intraplate seismicity models where ruptures partially deplete a long-lived ‘pool’ of lithospheric stress, triggered by transient stress perturbations (Calais *et al.*, 2016; Chéry & Vernant, 2006; Clark, 2010; Liu & Stein, 2016; So & Capitanio, 2016).

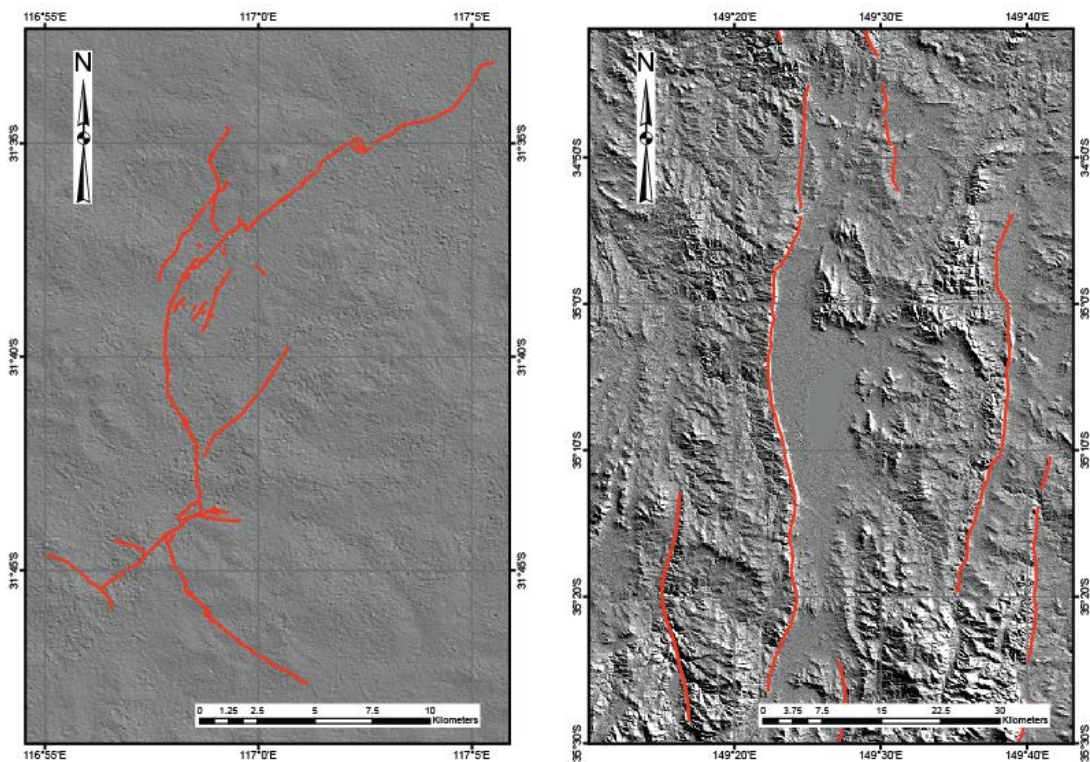


Figure 2: Cratonic versus non-cratonic rupture characteristics. (A) the ‘one-off’ 1968 Ms6.8 Meckering scarp, (B) the pre-historic ~200 m high Lake George fault scarp.

There have been no earthquakes associated with surface rupture in the non-cratonic and extended parts of Australia in historic times, and Holocene ruptures are yet to be discovered. This is despite abundant evidence for strain localization on Quaternary-active faults in these crustal types. Total Pliocene to Quaternary uplift across individual structures can be up to several hundred metres (Clark *et al.*, 2012; Figure 2b). Paleoseismological studies of key faults indicate that slip is not distributed evenly through time (Clark *et al.*, 2014a; Clark *et al.*, 2015; Clark *et al.*, 2012). Active periods lasting a few tens of thousands of years and involving a few tens of metres of uplift can be separated by hundreds of thousands to a million years of quiescence. Compared to cratonic areas, scarps are simpler in form (Figure 2b, perhaps partly an artefact of their age?), are longer (in some cases exceeding what might be expected of an Mmax rupture), and are arranged into networks and belts of Quaternary-active structures.

Maximum single event uplift values are in the order of 2 m and rarely up to 4-7 m. Work continues to define appropriate magnitude frequency distributions to describe rupture in 'active' periods. For example, might an Omori's law-style decay curve be more appropriate than a Gutenberg-Richter or Characteristic model (cf. Liu & Stein, 2016)?

Table 1: Historic events known to have produced surface rupture in Australia (after Clark *et al.*, 2014b).

Earthquake	Year	Magnitude (Mw)	SRL (km)	v.d. (max: m)
Meckering	1968	6.58	37	2.5
Calingiri	1970	5.46	3.3	0.4
Cadoux	1979	6.13	14	1.4
Marryat Creek	1986	5.74	13	0.9
Tennant Creek*	1988	6.76	36	1.8
Katanning	2007	4.73	1.26	0.1
Ernabella	2012	5.37	1.5	0.5
Petermann Ranges	2016	6.10	20	1.0

* The Tennant Creek surface rupture was produced by 3 events in a 24 hr period.

In this context, fault rupture displacement hazard might only meaningfully be defined in non-cratonic and extended parts of the continent where earthquake recurrence on individual structures is probable. Until a surface rupture is experienced in this setting, near field fault displacements and scarp complexity must be assessed using paleoscarp data, or through use of global analogues (e.g. Crone *et al.*, 1997). Developing an understanding of fault displacement hazard is important to Australia's sustainability and future development as the crustal types where fault rupture recurrence might be expected support the bulk of Australia's population and infrastructure.



© Commonwealth of Australia (Geoscience Australia) 2016

<http://creativecommons.org/licenses/by/4.0/legalcode>

REFERENCES

- Calais, E., Camelbeeck, T., Stein, S., Liu, M. & Craig, T.J. 2016. A New Paradigm for Large Earthquakes in Stable Continental Plate Interiors. *Geophysical Research Letters*, 10.1002/2016GL070815.
- Chéry, J. & Vernant, P. 2006. Lithospheric elasticity promotes episodic fault activity [rapid communication]. *Earth and Planetary Science Letters*, 243: 211-217.
- Clark, D. 2010. Identification of Quaternary scarps in southwest and central west Western Australia using DEM-based hill shading: application to seismic hazard assessment and neotectonics. *International Journal of Remote Sensing*, 31(23): 6297-6325.
- Clark, D., Dentith, M., Wyrwoll, K.H., Yanchou, L., Dent, V. & Featherstone, C. 2008. The Hyden fault scarp, Western Australia: paleoseismic evidence for repeated Quaternary displacement in an intracratonic setting. *Australian Journal of Earth Sciences*, 55: 379-395.

- Clark, D., McPherson, A. & Allen, T. 2014a. Intraplate earthquakes in Australia. In: P. Talwani (Editor), *Intraplate Earthquakes*. Cambridge University Press, New York, pp. 8-49.
- Clark, D., McPherson, A., Allen, T. & De Kool, M. 2014b. Co-seismic surface deformation relating to the March 23, 2012 MW 5.4 Ernabella (Pukatja) earthquake, central Australia: implications for cratonic fault scaling relations. *Bulletin of the Seismological Society of America*, 104(1): 24-39, doi: 10.1785/0120120361.
- Clark, D., McPherson, A., Collins, C. & Australia, G. 2011. Australia's seismogenic neotectonic record: a case for heterogeneous intraplate deformation. *Geoscience Australia*.
- Clark, D., McPherson, A., Cupper, M., Collins, C.D.N. & Nelson, G. 2015. The Cadell Fault, southeastern Australia: a record of temporally clustered morphogenic seismicity in a low-strain intraplate region. In: A. Landgraf, S. Kuebler, E. Hintersburger and S. Stein (Editors), *Geological Society, London, Special Publication Seismicity, Fault Rupture and Earthquake Hazards in Slowly Deforming Regions*.
- Clark, D., McPherson, A. & Van Dissen, R. 2012. Long-term behaviour of Australian Stable Continental Region (SCR) faults. *Tectonophysics* 566-567: 1-30, <http://dx.doi.org/10.1016/j.tecto.2012.07.004>.
- Crone, A.J., de Martini, P.M., Machette, M.N., Okumura, K. & Prescott, J.R. 2003. Paleoseismicity of Two Historically Quiescent Faults in Australia: Implications for Fault Behavior in Stable Continental Regions. *Bulletin of the Seismological Society of America*, 93: 1913-1934.
- Crone, A.J., Machette, M.N. & Bowman, J.R. 1997. Episodic nature of earthquake activity in stable continental regions revealed by palaeoseismicity studies of Australian and North American Quaternary faults. *Australian Journal of Earth Sciences*, 44: 203-214.
- Estrada, B. 2009. Neotectonic and palaeoseismological studies in the southwest of Western Australia, The University of Western Australia, Perth.
- Liu, M. & Stein, S. 2016. Mid-continental earthquakes: Spatiotemporal occurrences, causes, and hazards. *Earth Science Reviews*, 10.1016/j.earscirev.2016.09.016.
- Mooney, W.D., Ritsema, J. & Hwang, Y.K. 2012. Crustal seismicity and the earthquake catalog maximum moment magnitude (M_{cmax}) in stable continental regions (SCRs): Correlation with the seismic velocity of the lithosphere. *Earth and Planetary Science Letters*, 357-358: 78-83.
- So, B.-D. & Capitanio, F.A. 2016. The emergence of seismic cycles from stress feedback between intra-plate faulting and far-field tectonic loading. *Earth and Planetary Science Letters*, 447: 112-118, <http://dx.doi.org/10.1016/j.epsl.2016.05.002>.
- Talwani, P. 2014. Chapter 11. Unified model for intraplate earthquakes. In: P. Talwani (Editor), *Intraplate Earthquakes*. Cambridge University Press, United Kingdom, pp. 275-302.
- Whitney, B., Clark, D., Hengesh, J. & Bierman, P. 2015. Paleoseismology of the Mount Narryer fault zone, Western Australia: A multistrand intraplate fault system. *Geological Society of America Bulletin*, 10.1130/B31313.1.

Fault displacement hazard at natural gas storage fields-a future research and regulatory direction.

Thomas L. Davis
Geologic Maps Foundation, Inc.

Gas fields, Aliso leak, fault hazard, and regulatory direction: In the US over 400 natural gas storage fields supply nearly one-third of our nation's energy needs. That share is expected to grow in response to low-carbon fuel demands driven by climate change concerns, ample domestic supplies, and recent regulations. Natural gas (methane) provides fuel for electrical generation and heating and is often described as the low carbon bridge fuel from carbon intense coal and oil to renewables. While underground gas storage fields add flexibility to our energy system by providing ample supplies during periods of high demand they keep energy costs low by buying and storing during periods of low demand. As with most energy sources, natural gas comes with its own set of challenges: for example, the largest methane leak in US history recently occurred at the Aliso Canyon Gas Storage Field (ACGSF, aka Porter Ranch), California. Taking almost four months to control, the ACGSF leak demonstrated the difficulty of stopping an underground leak from one well in a pressured and large volume storage field. The leak underscores the need to evaluate all hazards and risks to gas storage fields and wells to avoid future environmental and societal damage, and the disruption of a needed source of energy and the waste of a valuable resource. The American Petroleum Institute RP 1171 (API 2015), that is guiding State of California and Federal new rule-making states "Depleted hydrocarbon reservoirs are candidates for natural gas storage because the reservoir integrity has been demonstrated over geologic time by hydrocarbon containment at initial pressure conditions." True, but gas wells at storage reservoirs have not existed over geologic time. A hazard such as fault displacement across a high pressure gas well during an earthquake could result in the rapid release of large volumes of methane to the atmosphere. If fault displacement is across many wells there is the potential for a methane release of much greater magnitude and difficulty to control than the recent leak at the ACGSF. In response to the ACGSF leak new recommendations, rulemaking, and policies for gas storage fields are being discussed and proposed at the industry advisory, State, and Federal levels in order to prevent the recurrence of such an event. While this direction is useful it is focused on well design and integrity, but a broader approach is needed where fault displacement hazard and risk are identified and evaluated. For example, in California several large gas storage fields, adjacent to urban areas, are developed across or close to potentially active faults capable of generating moderate to large earthquakes with up to several meters of fault displacement, yet the seismic risks to gas well integrity, the environment, and the nation's energy supply are poorly understood. Fault displacement hazard analysis (FDHA and PFDHA; Youngs, et al., 2003; Wells and Kulkarni, 2014) with its emphasis on the quantification of the distribution and variation of fault displacements, site-specific probabilistic analysis, design of infrastructure, and risk assessment could play a very important role in evaluating the safety of natural gas storage fields-if the approach is modified for the subsurface setting and gas well design. Incorporation of FDHA into risk evaluations of gas fields and wells will probably require changes in the State and Federal regulations given the past lack of attention to this hazard. For instance, there is no public record of the operator at ACGSF, the Southern California Gas Company, or the State regulators of wells and gas fields, the California Division of Oil & Gas (DOGGR) and the California Public Utilities Commission, recognizing or evaluating the fault displacement hazard to the gas storage field and wells by the Santa Susana fault (SSF). Yet the SSF's existence and location within the ACGSF

and prior oil field has been known to geologists since the late 1930s, and the California Geologic Survey's mapping shows that a segment of the fault, that is within a few kilometers of the field, ruptured the surface during the 1971 Sylmar earthquake (MW=6.4-6.7), and the surface segment of the fault closest to the ACGSF has had Holocene movement. This lack of attention is now addressed in proposed regulations by DOGGR that will require the operator to identify hazards and submit a risk management plan that includes mitigation, and adding FDHA could fill a key safety and environmental need. On the Federal level, the passage in June 2016 of the US PIPES Act provides a two year open window for technical input and to influence new nation-wide regulations being formulated by the Pipeline and Hazardous Material Safety Administration (PHMSA) for natural gas storage fields. Inclusion of FDHA into Federal regulations would provide a uniform environmental and safety standard across the nation. PHMSA already has regulations and guidelines for surface gas pipelines crossing potentially active faults (PHMSA, 2011) and extension of that role to the subsurface makes sense given the much more difficult work of controlling leaks from gas wells compared to surface pipelines.

ACGSF example: The ACGSF leak not only shows the impact of a lengthy, uncontrolled gas flow from just one well adjacent to an urban area (DOE, 2016), but it also focuses attention on the fault displacement hazard along the SSF (DOE, 2016, pg 61). It should be noted that the ACGSF leak is probably the result of casing corrosion pending on-going investigations and probably not due to movement on the SSF as no other wells crossing the SSF leaked, and there was no nearby earthquake at the initiation of the leak. Following are some of most significant impacts of the leak as of July 2016 (Harris and Walker, 2016): ~8,000 residents were relocated, ~ 5 Bcf of methane released to the atmosphere, operator has spent \$550 MM dealing with the leak, 25 + class action suits against the operator were active, and the substantial cost of the lost commodity (methane). During the leak numerous surface control attempts failed (top kills) and aggravated the leak that went from 2.0 to 25-60 MMcfd (DOE, 2015), and the leak was finally stopped by a relief well that took over two months to drill.

The Santa Susana fault displacement hazard: The conclusion that the SSF is a displacement hazard at the ACGSF is based on the following (Davis, 2016): 1) All of the 114 Aliso Canyon gas storage wells that were active in 2015 intersect the SSF. 2) Many of the fault intersections are at shallow depths (less than 500 m below the surface) and there are several potential conduits for gas migration to the surface from a damaged high pressure gas well: the strata from just above the SSF to the surface are highly-fractured and dominated by vertical fracture sets; the SSF zone is a thick band of shear-fractures that comes to the surface near the Porter Ranch community; and the Aliso leak showed that gas can flow to the surface just outside of the well casing. 3) The California Geologic Survey (CGS) recognizes, via the Alquist-Priolo Act (AP), that the SSF's eastern segment is an earthquake and fault-rupture hazard based on surface offset during the 1971 Sylmar earthquake. 4) The various slip rate estimates for the SSF are high. The 2015 Third Uniform California Earthquake Rupture Forecast, or "UCERF3," slip average is 2.9 mm/yr for the SSF. Yeats (2001) concludes the SSF has had 4.9-5.9 km of slip during the last 600,000-700,000 years that yields the exceptionally high slip-rate of 7.0-9.8 mm/yr (roughly 1/3 to 1/2 the convergence rate of the entire western Transverse Ranges, Namson and Davis, 1988). 5) Additionally to the west and east the SSF merges with the active Oak Ridge and Sierra Madre faults respectively. The recurrence time of fault movement on the SSF is presently unclear due to its poor surface exposure, extensive landslide deposits covering much of the fault zone, a wide and complex shear zone with two major splays, and limited fault trenching-all of which constrain surface-based paleoseismic knowledge.

Mitigation: DOGGR's proposed rulemaking requires the operator to submit a risk management plan that includes risk mitigation. In general the mitigation options are limited at ACGSF and probably at other gas fields subject to fault displacement hazard: 1) As demonstrated by the ACGSF leak there is no quick and easy way to draw-down the pressure and volume of a gas storage field that has a sizable downhole leak. 2) Control of the leaking well (SS-25) took over two months, and required drilling of a relief well and a backup well. 3) Installation of downhole shut-off valves (DHSVs) on wells have been proposed at the ACGSF and other fields but the reliability of these valves is unclear especially during a nearby earthquake, and DOE and DOT have recommended doing a cost and benefit analysis of DHSVs (DOE, 2016). 4) The location of the ACGSF adjacent to urban areas of Los Angeles increases the societal impact if SSF displacement and well shearing occur plus adding an enormous legal and financial obligation to the operator.

Summary and Policy: Society can't fix a problem by ignoring or discounting it and now is the time for the geologic community to influence new regulations being considered for the safety of gas storage fields and wells. The SSF is a recognized and regulated fault rupture hazard at the surface with a high slip rate, and if the SSF is a rupture hazard at the surface it is also a rupture hazard in the subsurface. All of the wells at the ACGSF cross the SSF and their shallow fault intersections might allow for a massive gas leakage to the surface if SSF displacement were to shear the wells. A FDHA is needed for proper fault risk assessment and mitigation plans at the ACGSF. The California Geologic Survey via the Alquist-Priolo Act regulates surface construction on and near potentially active surface faults in California and that statutory and regulatory role should be extended to subsurface fault rupture hazards. The new DOGGR Discussion Draft that identifies active faults as a hazard to gas storage wells is an important step. The California Public Utilities Commission (CPUC) regulates gas utilities' transmission and distribution pipeline systems that includes gas storage fields but its regulatory role in regard to fault displacement hazard is unclear. API RP 1171 (API, 2015) is useful but should be revised to include more guidance about fault displacement hazard and risk in seismic prone regions. PHMSA does not currently have regulations addressing underground storage, but has statutory authority over interstate and intrastate underground storage facilities (PHMSA, 2011). The 2016 PIPES Act requires PHMSA to issue, within two years, minimum safety standards for underground natural gas storage facilities. The Act allows states to adopt more stringent safety standards for intrastate facilities, if such standards are compatible with the minimum standards prescribed in the Act. Seismically active states like California should adopt standards dealing with the fault displacement risk at gas storage fields that require implementation of FDHA even if they are above the future minimum federal standards. Regulators and operators will find FDHA useful in determining whether it is safe to site gas storage fields across or near potentially active faults and reassuring the public of their decisions. Finally, there is an important role for petroleum geologists and the oil and gas industry to play in fault displacement hazard analysis and regulatory advice for gas storage fields and more broadly for earthquake hazards evaluations by virtue of their unique subsurface expertise and familiarity with deeper data sets and modern mapping and structural techniques.

References:

API, 2015, American Petroleum Institute, Functional Integrity of Natural Gas Storage in Depleted Hydrocarbon Reservoirs and Aquifer Reservoirs, API Recommended Practice 1171, First Edition, September, 2015.

Davis, T.L., 2016, The Santa Susana fault, Aliso Canyon gas storage field, southern California: possible fault rupture hazard, gas well integrity, and regulatory implications (abstract): Joint Annual Meeting of Pacific and Rocky Mountains Sections American Association of Petroleum Geologists (AAPG) Las Vegas, NV, October 2-5, 2016.

DOE (Department of Energy), 2016, Results of Federal Task Force: Ensuring Safe and Reliable Underground Natural Gas Storage Final Report of the Interagency Task Force on Natural Gas Storage Safety.

Harris, K., and Walker, A., 2016, California Division of Oil, Gas, & Geothermal Resources (DOGGR) Response to Aliso Canyon Gas Leak, US DOE National Laboratories Workshop on Well Integrity for Natural Gas Storage in Depleted Reservoirs and Aquifers, Broomfield, CO, July 12-13, 2016.

Namson, J.S. and Davis, T.L., 1988, Structural transect of the western Transverse Ranges, California: implications for lithospheric kinematics and seismic risk evaluation: *Geology*, v.16, p.675-679.

PHMSA, 2011, Pipeline and Hazardous Material Safety Administration (DOT-Department of Transportation), 49 CFR (Code of Federal Regulations) 192.900 series, Subpart O—Gas Transmission Pipeline Integrity Management, 2011 edition.

Wells, D.L., and Kulkarni, V.S., 2014, Probabilistic and Deterministic Fault Displacement Hazard Analysis—Sensitivity Analyses and Recommended Practices for Developing Design Fault Displacements, Proceedings of the 10th National Conference in Earthquake Engineering, Earthquake Engineering Research Institute, Anchorage, AK.

Yeats, R.S., 2001, Neogene tectonics of the east Ventura and San Fernando basins, California: an overview: in T.L. Wright and R.S. Yeats eds., *Geology and tectonics of the San Fernando Valley and east Ventura basin, California*, Pacific Section American Association of Petroleum Geologists, Guidebook 77, p. 9-36.

Youngs, R.R., et al., 2003, A methodology for probabilistic fault displacement hazard analysis (PFDHA), *Earthquake Spectra*, v. 19, no. 1, pgs 191-219.

Fault rupture observations from the most recent and prior events along New Zealand's Alpine and Greendale Faults

Gregory De Pascale
Department of Geology and CEGA
University of Chile, email: snowyknight@gmail.com

New Zealand (NZ) is actively deforming and on September 4, 2010 the previously unknown and slow-slipping Greendale fault ruptured during the Mw 7.1 Darfield earthquake and NZ observed its first 21st Century surface rupture. This rupture was the first of a series of perhaps interconnected major earthquakes and surface ruptures along dextral and reverse faults along the Eastern South Island (2010 to present) leading to the major November 2016 Mw 7.8 Cheviot earthquake (~120 km away from 2010's Darfield event). Although analysis of this most recent event is currently underway, much can be learned through observations from the Greendale fault and along the fast-slipping nearby plate boundary Alpine fault. Importantly, although the Alpine fault is NZ's fastest slipping crustal fault, it appears to have not had a surface rupture since 1717 (~300 years; Wells et al., 1999). A combination of a recent rupture (i.e. the Greendale fault) and improving technology and methods (e.g. lidar), combined with field mapping along previous ruptures provides us with informative examples to better understand fault displacement hazards.

The dextral-reverse Alpine Fault on the South Island of NZ is the clear onshore manifestation of this plate boundary (Wellman, 1953) and accommodates 50-90% of the 39.7 ± 0.7 mm/yr relative motion across the plate boundary (De Mets et al., 2010; Sutherland et al., 2007) along its central and southern sections (Norris and Cooper, 2001; Barnes, 2009). It has the largest documented displacements of bedrock terranes on Earth (Lamb et al., 2016) with ~700 km over 25 Ma (or ~28 mm/yr). Prior to this work (e.g. De Pascale and Langridge, 2012; De Pascale et al., 2014; De Pascale et al. In Revision), there was little known about surface rupture characteristics and widths of deformation partially due to difficult terrain and extensive temperate rainforest cover. Digital topography is critical to our increased understanding of the Alpine fault. A digital elevation model (DEM) was derived from a 34 km-long, one kilometer-wide, airborne lidar survey flown in 2010 (Langridge et al., 2014). Fault traces and geomorphology were mapped using this DEM. Details on the collection, processing, and metadata of this dataset are outlined in Langridge et al. (2014). Analysis of these lidar-derived digital topography data combined with field observations allowed the discovery and quantification of previously unrecognized dextral offsets (De Pascale et al., 2014). The average surface dextral displacements (along one main fault trace) during the most recent event (in 1717) was 7.1 ± 2.1 m, and through a compilation of all of the published offsets along the alpine show consistent offsets of ~ 5 to 9 m along a minimum of 380 km section of the fault (Wells et al., 1999; De Pascale and Langridge, 2012; De Pascale et al., 2014). Based on data limitations and uncertainties regarding dextral offsets, the possibility that smaller ruptures (moderate to large partial ruptures) along the fault cannot be ignored, but that larger displacements (from 5 to 9 m dextral) should be expected. Regarding widths of deformation along the Alpine fault, again the lidar DEM dataset is of huge value. Near the Whataroa River, through a combination of DEM analysis (i.e. profiling and mapping) combined with field observations, the Alpine fault has multiple, sub-parallel active traces that are ~250-300 m apart at the surface (De Pascale et al., In Revision). Deformation along these traces appear quite localized, however due to the resolution of the lidar data, having additional traces that do not carry significant slip, but are present between the main traces of the fault is possible. Uplift appears to be accommodated along the outboard thrust-related traces along the Alpine fault and most of the strike-slip deformation occurs along inboard traces. Because of uncertainties in the data, due to dense vegetation and cover of fault traces by debris-flows and alluvium, defining a first-order fault displacement exclusion zone (i.e. where the potential for surface ruptures is extremely low) would be within a zone no less than 500 wide along the Alpine fault based on this new analysis. Due to the Southern Alps range-front bounding nature of the Alpine fault, and based on the extensive expected landslides and rockfall here (Robinson et al., 2016), the overall hazard along the range-front of the Southern Alps is both from surface rupture hazards along the fault in addition to rockfall, landslides,

debris flows and rock avalanches that will certainly impact much of the area surrounding active Alpine fault traces.

During field mapping along the Alpine fault, the first outcrop and scarp of the South Westland Fault Zone (SWFZ), a system of northwest-west vergent reverse/thrust faults in the footwall of the Alpine fault, was discovered (De Pascale et al., 2016). Although the SWFZ is 300 km long and has evidence for 3500 m of dip-slip displacement it was unknown if it was active. Though a combination of structure from motion (SfM), combined with scarp profiling using a GPS and total station surveying of key units allowed important insight into key fault displacement hazards. Importantly the displacement from the most recent event at this site is $1.2 \text{ m} \pm 0.1 \text{ m}$ ($0.5 \text{ m} \pm 0.1 \text{ m}$ throw) alluvium thrust over the youngest silt overbank (or loess) deposit. The alluvium overthrusting silt near the top of the exposure is coincident with the up to the southeast $\sim 0.7 \text{ m}$ to 1.1 m high scarp (possibly degraded from farming) along the terrace at the top of the exposure. Finally our survey of the unit contacts shows gentle anticlinal, hanging wall folding within 170 m of the scarp and demonstrates the combination of folding and faulting as hazards in thrust faults adjacent to the Alpine fault.

Greendale fault ruptured in September 2010 during the Mw 7.1 Darfield earthquake and generated a 29.5 ± 0.5 -km-long surface rupture (Quigley et al., 2012) as observed from lidar-derived topography with surface ruptures displacing a number of linear features (hedgerows, roads and railroads), in addition to houses and provided excellent markers for displacements. InSAR line-of-sight displacement field indicated a rupture of around 45 km (Elliott et al., 2012). Fault-zone trapped waves (FZTWs) recorded from a seismic array crossing and on the Greendale fault suggests that the Greendale fault rupture zone is up to 200-250 m wide (Li et al., 2014) and is consistent with surface deformation width (e.g. Quigley et al., 2012). Maximum dextral displacements were $5.3 \pm 0.5 \text{ m}$ with average dextral displacements of $2.5 \pm 0.1 \text{ m}$ based on field and lidar data (which are $\sim 25\%$ greater than expected than regressions would suggest, e.g. Wells and Coppersmith, 1984; Wesnousky, 2008, which means that the shorter surface rupture here produced larger displacements than expected), with a width of deformation from 30 to 300 m wide (Quigley et al., 2012).

Finally, although not often considered as part of a fault displacement hazards, the headscarps of lateral spreads (i.e. normal faults), which were extremely common during the main aftershocks of the Darfield Earthquake (including the Feb 2011 Christchurch NZ Earthquake) and are a coseismic phenomena, deserve mention. These steeply dipping normal faults were observed at a number of sites within Christchurch with major impacts on infrastructure built over these incipient headscarps. Because these lateral spreads form normal faults at their upslope margins, and because these normal faults form displacement hazards, these “special case” faults should be also considered in regards to rupture displacement hazard. Although they form due to slope stability reduction during lateral spreading due to liquefaction, these displacement hazards are not currently well-represented in either the lateral spreading literature (or guidelines; e.g. the 2016 NZ Guidelines for Earthquake Engineering) or within the fault displacement literature, but should be considered, certainly for critical facilities or for lifelines.

Importantly two of the NZ faults mentioned here (i.e. the Greendale and SWFZ) were poorly mapped or unknown prior to a recent rupture or field identification. It therefore prudent to recall that *it is impossible to understand fault displacement hazards along a fault zone if the fault zone is unknown or poorly mapped*. In particular areas where geomorphic surfaces are modified through human use (e.g. farming in Canterbury or perhaps California's or Chile's Central Valleys), or are obscured due to dense vegetation (e.g. parts of NZ, the Pacific Northwest of North America, Indonesia or Patagonia) there are likely faults with displacement hazards that are under appreciated. Better mapping both in the field and when using lidar data in places where vegetation is an issue, SfM data (when vegetation is not an issue), and combined with subsurface geophysical data may provide insight into the presence or absence of potentially active faults. After these are identified, further fault characterisation can take place. In terms of pitfalls regarding fault displacement hazards, besides not mapping or acknowledging potentially active faults, if we overestimate slip-rates and displacement hazards along some structures

that we know to be active, than we may be underestimating the hazard posed by adjacent and perhaps low-recurrence (although active) faults. This ultimately reminds us that if we stay focused on the big players (e.g. Alpine or San Andreas faults), we may miss the lower-recurrence but also high-consequence ruptures along subsidiary faults.

Acknowledgements

This research was funded by the NZ Geoscience Society's Wellman Research Award, the NZ Earthquake Commission (EQC), a UChile FCFM Initiation Grant, and Chilean FONDECYT Project 11160038. Lateral Spread research in Christchurch funded by a NSF Grant (Remote Sensing of Lateral Spread Displacements) to Ellen Rathje.

References

- Barnes, P.M., 2009, Postglacial (after 20 ka) dextral slip rate of the offshore Alpine fault, New Zealand: *Geology*, v. 37, p. 3–6, doi:10.1130/G24764A.1.
- DeMets, C., Gordon, R.G., Argus, D.F., and Stein, S., 1994, Effect of recent revisions to the geomagnetic reversal time scale on estimates of current plate motions: *Geophysical Research Letters*, v. 21, p. 2191–2194, doi:10.1029/94GL02118.
- De Pascale, G.P., and Langridge, R., 2012, New on-fault evidence for a great earthquake in A.D. 1717, central Alpine fault, New Zealand: *Geology*, v. 40, p. 791–794, doi:10.1130/G33363.1.
- De Pascale, G. P., Davies, T. R., and M.C. Quigley, 2014, Lidar reveals uniform Alpine Fault offsets and bimodal plate boundary rupture behavior, *New Zealand, Geology*, 42(5), 411-414, Doi:10.1130/G35100.1.
- De Pascale, G. P., N. Chandler-Yates, F. Dela Pena, P. Wilson, E. May, A. Twiss, and C. Cheng (2016), Active tectonics west of New Zealand's Alpine Fault: South Westland Fault Zone activity shows Australian Plate instability, *Geophys. Res. Lett.*, 43, doi:10.1002/2016GL068233.
- De Pascale, G.P., Duffy, B., Klahn, A., and Davies, T.R.H., *Under Revision*, Alpine Fault deformation and hanging-wall tectonic uplift characterised from lidar-derived DEM mapping combined with OSL dating, Whataroa River, New Zealand: *Journal of Geophysical Research – Solid Earth*.
- Elliott, J. R., E. K. Nissen, P. C. England, J. A. Jackson, S. Lamb, Z. Li, M. Oehlers & B. Parsons, 2012, Slip in the 2010–2011 Canterbury earthquakes, New Zealand, *Journal of Geophysical Research*, v. 117, B03401.
- Lamb, S., N. Mortimer, E. Smith, and G. Turner (2016), Focusing of relative plate motion at a continental transform fault: Cenozoic dextral displacement >700 km on New Zealand's Alpine Fault, reversing >225 km of Late Cretaceous sinistral motion, *Geochem. Geophys. Geosyst.*, 17, doi:10.1002/2015GC006225.
- Langridge, R. M., Ries, W. F., Farrier, T., Barth, N. C., Khajavi, N., and G. P. De Pascale, 2014, Developing a sub 5-m lidar DEM for forested sections of the Alpine and Hope faults, South Island, New Zealand: Implications for structural interpretations, *Journal of Structural Geology*, 64, 53-66.
- Li, Y-G., De Pascale, G.P., Quigley, M., Gravely, D., 2014, Fault Damage Zones of the M7.1 Darfield and M6.3 Christchurch Earthquake Sources Viewed with Fault-Zone Trapped Waves, *Tectonophysics* v. 618, p.79-101.
- Norris, R.J., and Cooper, A.F., 2001, Late Quaternary slip rates and slip partitioning on the Alpine Fault, New Zealand: *Journal of Structural Geology*, v. 23, p. 507–520, doi:10.1016/S0191-8141(00)00122-X.
- Quigley, M., Van Dissen, R., Litchfield, N., Villamor, P., Duffy, B., Barrell, D., Furlong, K., Stahl, T.,

Bilderback, E., and Noble, D., 2012, Surface rupture during the 2010 Mw 7.1 Darfield (Canterbury, New Zealand) earthquake: Implications for fault rupture dynamics and seismic-hazard analysis: *Geology*, v. 40, p. 55–58, doi:10.1130/G32528.1.

Robinson, T.R., Davies, T.R.H., Wilson, T.M. And C. Orchiston, 2016, Coseismic landsliding estimates for an Alpine Fault earthquake and the consequences for erosion of the Southern Alps, New Zealand. *Geomorphology*, 263, 71-86.

Sutherland, R., and 18 others, 2007, Do great earthquakes occur on the Alpine fault in central South Island, New Zealand? *in* Okaya, D., Stern, T.A., and Davey, F., eds., *A Continental Plate Boundary: Tectonics at South Island, New Zealand*, Geophysical Monograph Series, Washington, D.C., American Geophysical Union, p. 235– 251.

Wellman, H.W., 1953, Data for the study of Recent and late Pleistocene faulting in the South Island of New Zealand: *New Zealand Journal of Science and Technology*, v. 34B, p. 270–288.

Wells, A., Yetton, M.D., Duncan, R.P., and Stewart, G.H., 1999, Prehistoric dates of the most recent Alpine fault earthquakes, New Zealand: *Geology*, v. 27, p. 995–998, doi:10.1130/0091-7613(1999)027<0995:PDOTMR>2.3.CO;2.

Wells, D.L., and Coppersmith, K.J., 1994, New Empirical Relationships among Magnitude, Rupture Length, Rupture Width, Rupture Area, and Surface Displacement, *Bulletin of the Seismological Society of America*, V. 84, N. 4, p. 974-1002.

Wesnousky, S. G., 2008, Displacement and geometrical characteristics of earthquake surface ruptures: Issues and implications for seismic-hazard analysis and the process of earthquake rupture, *Bull. Seismol. Soc. Am.*, v. 98, p. 1609–1632, doi:10.1785/0120070111.

A New Technique to Measure 3D Slip Vectors from High-resolution Topography, Applied to Photogrammetry of Historic Ruptures

Austin Elliott¹, David Mackenzie¹, Barry Parsons¹, Zhikun Ren²

¹Centre for Observation and Modelling of Earthquakes, Volcanoes and Tectonics, University of Oxford, UK

²Institute of Geology, China Earthquake Administration, Beijing, China

The modern prevalence of high resolution digital topography offers literally a new dimension in our ability to measure geomorphic fault displacements. Not only can we detect distributed strain and off-fault deformation from 2-dimensional maps of displacement fields, but full 3D representations of offset markers provide constraints on feature reconstruction that improve the quality and may increase the number of discrete offset measurements along a fault surface-rupture. Conventional methods of measuring offsets using linear markers and topographic profiles face severe limitations when faults dip shallowly, or when the slip vector and/or fault attitude are highly oblique to the topographic surface. We present a new method to measure 3D displacement vectors that exploits the sensitivity of offset measurements to surface orientation and fault attitude, even in the absence of clear piercing points. We employ photogrammetrically derived high-resolution digital elevation models to map detailed, well preserved surface breaks from two historic earthquakes in Central Asia-- the 1932 M7.6 Changma earthquake in western China, and the 1889 M8.3 Chilik earthquake in southern Kazakhstan. We use this new method of measuring orthogonal offsets of multiple adjacent surfaces to measure the ratio of vertical to horizontal fault slip at sites along these ruptures where individual piercing points are absent or only weakly defined.

The conventional use of topographic profiles to measure vertical fault offset (fault throw) relies on a set of assumptions that consider a few common factors negligible: the absence of oblique slip, the coincidence of slope direction and fault normal or slip direction, and a modest topographic slope. Similarly, measurements of horizontal offset rely largely on 1-dimensional linear features that produce singular piercing points, constraining only the component of slip orthogonal to the feature in question unless fault attitude is independently known and fault-normal motion is accounted for. In traditional geomorphic studies of fault slip, sites are preferentially selected that roughly adhere to these simplifying assumptions (e.g., investigators often avoid measurement of offset at sites that suffer from unknown fault geometry or high feature-to-fault obliquity), curtailing the amount of data that can be easily collected using conventional methods. High resolution digital topography affords us the ability to 1) constrain the uncertainty in measured offset introduced by the confounding effects of slope-fault-offset geometry, and 2) measure more robust feature displacements in three dimensions using the apparent offsets of multiple markers on a single geomorphic feature.

Mackenzie and Elliott (in review) presents analytical comparisons of fault throw measured from 2D profiles versus real fault throw for a variety of fault–slope–slip-vector configurations. The resulting relative errors, plotted in dip–rake–hillslope-angle parameter space, illustrate the sensitivity of 2D offset measurements to the relative geometries of the fault, the topographic surface, and the slip vector. These results formalize the permissible boundaries of fault dip, surface aspect, and oblique slip ratio from which profiles can be measured that will not be

contaminated beyond a given uncertainty by geometric artifacts. Within this framework we develop a Monte-Carlo analysis of uncertainties in fault, slope, and slip geometry which we propose should accompany any slip measurement made from a 2D topographic profile.

We can expand our offset-measurement methodology beyond two dimensions, however, by exploiting the change in apparent offset with changing marker geometry along a fault. Ambiguities in oblique offset or from oblique surface-fault geometry may be eliminated by incorporating apparent offsets measured on multiple different sides of a landform. Combining multiple pairs of correlative offset surfaces that represent different parts of the same landform (e.g., different flanks of a moraine, banks of a channel, or local faces of a conical alluvial fan) can uniquely define the offset vector in three dimensions. Each individual offset surface pair gives only the component of separation orthogonal to the surface, but if the slip vector is assumed to be uniform across the feature of interest, differently oriented offset surfaces on the same feature will incrementally constrain the offset in additional dimensions. We developed a method that calculates a 3D slip vector based on three or more pairs of correlative offset surfaces imaged with high resolution topography. We propose using this approach where the assumptions of conventional, profile-based offset measurement methods are violated.

The efficacy of the method is illustrated by comparison to contemporary studies of recent large surface rupturing earthquakes, and I show how the approach may be applied to measurements of fault slip of any age with examples from the enigmatic historical Central Asian earthquake ruptures of 1889 and 1932. Recent high-resolution satellite imagery permits detailed mapping of these fault ruptures. Despite well preserved traces and large scarps, each of these earthquakes exhibits a confounding variety of slip senses. In the absence of independently known fault attitudes and slip sense, measuring offsets requires our inherently 3D approach to account for unknown amounts of convergence and the ambiguity between surface aspect and oblique-lateral slip.

We encourage the use of this full geometric uncertainty analysis for measurements of fault throw from profiles across faults with any sense of obliquity, and we recommend measuring multiple related surface offsets instead of individual line-markers when simple geometric assumptions are violated.

References:

Mackenzie, D., and Elliott, A., (in review), Untangling Tectonic Slip from the Misleading Effects of Landform Geometry, *Geosphere*.

Case Study of the Analysis and Design of Bridge Foundations Intersected by Active Faulting

James Gingery
Kleinfelder

A case study involving the performance based analysis and design of rail road bridge foundations intersected by active faulting is presented. The basis for the surface fault rupture design scenarios is briefly discussed, including paleoseismic field investigations, and deterministic and probabilistic fault displacement hazard analyses. Analyses were conducted using three-dimensional nonlinear finite difference numerical models that were inclusive of all the bridge foundations, the soils and rock in the vicinity of the foundations, and the fault traces. Offsets were applied at the model boundaries pseudo-statically, and the resulting soil and pile responses were calculated. The pile response was sensitive to the depth at which the fault intersected the pile, with the most severe loading occurring when the fault passed within approximately the middle 1/3 of the pile length. The analysis showed that the CIDH piles were capable of undergoing significant ductility while maintaining support of the bridge loads without collapse. Observations are made on the challenges of applying FDHA results in foundation engineering.

Framework of probabilistic and deterministic methods for evaluating near-fault displacement

Inoue, N.¹, Tonagi, M.², Takahama, T.², Matsumoto, Y.², Kitada, N.¹, Dalguer, Luis A.³ and Irikura, K.³

¹Geo-Research Institute (GRI), Osaka, Japan

²Kozo Keikaku Engineering, Inc. (KKE), Tokyo, Japan

³Aichi Institute of Technology (AIT), Toyota, Japan

E-mail contact of main author: naoto@geor.or.jp

1 Introduction

In IAEA Specific Safety Guide (SSG)-9 (INTERNATIONAL ATOMIC ENERGY AGENCY, 2010), section 8.10 describes that probabilistic methods for evaluating fault displacement should be used if no sufficient basis is provided to decide conclusively that the fault is not capable by using the deterministic methodology described in section 8.3-8.7. In addition, International Seismic Safety Centre (ISSC) published it as ANNEX of Safety Reports Series No. 85 (Ground Motion Simulation Based on Fault Rupture Modelling for Seismic Hazard Assessment in Site Evaluation for Nuclear Installations: IAEA, 2015) to realize seismic hazard for Nuclear Installations described in SSG-9 and shows the utility of the deterministic and probabilistic evaluation methods for fault displacement in the annex of the safety report. In the SSG-9, two types of fault displacement are introduced: primary fault and secondary fault displacements. In Japan, New Regulatory Requirements (Nuclear Regulation Authority, NRA) require that important nuclear facilities shall be established on ground where fault displacement will not arise when earthquakes occur in the future. In other words, nuclear facilities important to seismic safety have been prohibited from constructing on the ground with occurrence of fault displacement. Therefore, it is important to obtain the-state-of-art knowledge on fault displacement. Under these situations, we need to develop the evaluation methods for fault displacement of primary and secondary faults. We are studying deterministic and probabilistic evaluating methods to evaluate the fault displacements based on tentative analyses of observed records such as surface earthquake faults and near-fault strong ground motions from inland crustal earthquake accompanied by fault displacements.

2 Deterministic Evaluation Approach

We attempt to estimate fault displacements using slip distributions on source faults dynamically evaluated based on a characterized source model explaining observed near-fault broad band ground motions. First, the characterized source models are estimated with forward modeling using empirical Green's function method and theoretical method (IAEA, 2015). Second, slip distributions on source faults are dynamically evaluated based on the characterized source models. The validity of dynamically constructed slip distributions are examined by comparison of observed waveforms and synthetic waveforms estimated by dynamic simulation. Referring the dynamically constructed slip distributions, we study an evaluation method for surface fault displacement using finite element method and hybrid method, which combines particle method and distinct element method. For an example, we show the result tentatively developed for the 1999 Chi-Chi earthquake.

3 Probabilistic Evaluation Approach

In the probabilistic evaluation approach, Probabilistic Fault Displacement Hazard Analysis (PFDHA), there are two types of fault displacement related to the earthquake fault: principal fault

displacement and distributed fault displacement. As mentioned above, distributed fault displacement should be evaluated in important facilities, such as Nuclear Installations. Youngs et al. (2003) defined the distributed fault as fault displacement on other faults or shears, or fractures in the vicinity of the principal rupture in response to the principal faulting. Other researchers treated the data of distributed fault around principal fault and modeled according to their definitions (e.g. Petersen et al., 2011; Takao et al., 2013, 2014). Their distributed fault displacement data exclude some kind of displacement, such as triggered displacement, landslide, from secondary fault displacement described in the SSG-9. We compiled fault displacement in and around Japan and constructed the slip-distance relationship depending on fault types.

4 Concluding Remarks

In the current status, the results of the numerical simulation show the surface stress change strongly depends on the geometry of the fault and the physical property of surface materials. In the result of the PFDHA, slip-distance relationship of distributed fault displacement (reverse fault) on the foot-wall indicated difference trend compared with that on hanging-wall, although the fault displacement data in PFDHA are sparse because we arrange fault displacement data into each mechanism. We will integrate the both results to better understand the distributed fault displacement in the future.

Acknowledgment: This research was part of the 2014-2015 research project 'Development of evaluating method for fault displacement' by the Secretariat of Nuclear Regulation Authority (S/NRA), Japan.

[1] International Atomic Energy Agency (2010) Seismic Hazards in Site Evaluation for Nuclear Installations, IAEA Safety Standards Series, No. SSG-9, Vienna: INTERNATIONAL ATOMIC ENERGY AGENCY.

[2] International Atomic Energy Agency (2015) Ground Motion Simulation Based on Fault Rupture Modelling for Seismic Hazard Assessment in Site Evaluation for Nuclear Installations, IAEA Safety Reports Series, No. 85, Vienna: INTERNATIONAL ATOMIC ENERGY AGENCY.

[3] Youngs, Robert R., Arabasz, Walter J., Anderson, R. Ernest, Ramelli, Alan R., Ake, Jon P., Slemmons, David B., McCalpin, James P., Doser, Diane I., Fridrich, Christopher J., Swan, Frank H., Rogers, Albert M., Yount, James C., Anderson, Laurence W., Smith, Kenneth D., Bruhn, Ronald L., Knuepfer, Peter L. K., Smith, Robert B., dePolo, Craig M., O'Leary, Dennis W., Coppersmith, Kevin J., Pezzopane, Silvio K., Schwartz, David P., Whitney, John W., Olig, Susan S., and Toro, Gabriel R. (2003) A Methodology for Probabilistic Fault Displacement Hazard Analysis (PFDHA), *Earthquake Spectra*, Vol. 19, No. 1, pp. 191-219.

[4] Petersen, Mark D., Dawson, Timothy E., Chen, Rui, Cao, Tianqing, Wills, David P.; Frankel Arthur D. Petersen Mark D., Christopher J.; Schwartz, Dawson, Timothy E., Chen, Rui, Cao, Tianqing, Wills, Christopher J., Schwartz, David P., and Frankel, Arthur D. (2011) Fault displacement hazard for strike-slip faults, *Bulletin of the Seismological Society of America*, Vol. 101, No. 2, pp. 805-825.

[5] Takao, Makoto, Tsuchiyama, Jiro, Annaka, Tadashi, and Kurita, Tetsushi (2013) Application of Probabilistic Fault Displacement Hazard Analysis in Japan, *Journal of Japan Association for Earthquake Engineering*, Vol. 13, No. 1, pp. 17-32.

[6] Takao, Makoto, Ueta, Keiichi, Annaka, Tadashi, Kurita, Tetsushi, Nakase, Hitoshi, Kyoya, Takashi, and Kato, Junji (2014) Reliability Improvement of Probabilistic Fault Displacement Hazard Analysis, *Journal of Japan Association for Earthquake Engineering*, Vol. 14, No. 2, pp. 2 16-2 36.

Quantifying Co-seismic Distributed Deformation Using Optical Image Correlation: Implications For Empirical Earthquake Scaling Laws And Safeguarding The Built Environment

Christopher Milliner

University of California, Berkeley

Measurements of co-seismic deformation from surface rupturing events are an important source of information for faulting mechanics and seismic hazard analysis. However, direct measurements of the near-field surface deformation pattern have proven difficult. Traditional field surveys typically cannot observe the diffuse and subtle inelastic strain accommodated over wide fault-zones, while InSAR data typically decorrelates close to the surface rupture due to high phase gradients leaving 1-2 km wide gaps of data. Using sub-pixel, optical image correlation of pre- and post-event air photos, we quantify the near-field, surface deformation pattern of the 1992 $M_w = 7.3$ Landers and 1999 $M_w = 7.1$ Hector Mine earthquakes. This technique allows spatially complete measurement of the surface co-seismic slip along the entire surface rupture, as well as the magnitude and width of distributed deformation. For both events we find our displacement measurements are systematically larger than those from field surveys, indicating the presence of significant distributed, 'off-fault' deformation. Here we show that the Landers and Hector Mine earthquakes accommodated 46% and 38% of displacement away from the main primary rupture as off-fault deformation, over a mean shear width of 154 m and 121 m, respectively, with significant spatial variability. We also find positive, yet weak correlations of the magnitude of distributed deformation with the type of near-surface lithology and degree of macroscopic fault zone complexity. We envision additional measurements of future ruptures will better constrain what physical properties of the surface rupture are important controls on the distribution of strain, necessary in order to reliably estimate the amount of expected distributed shear along a given fault segment. Our results have basic implications for the accuracy of empirical scaling relations of earthquake surface ruptures derived from field measurements, understanding apparent discrepancies between geologic-geodetic fault slip rates, and developing effective micro-zonation protocols for the built environment.

Surface Rupture Data and Location Uncertainty in Probabilistic Fault Displacement Hazard Analyses

Mark Petersen
U.S. Geological Survey

Rui Chen
California Geological Survey

We summarize data, methods, and models developed for probabilistic fault displacement hazard analyses (PFDHA). We compare earthquake displacement data and empirical fault displacement models that have been developed for normal, strike-slip, and reverse faults. In general the data and models are similar near the center of the fault for the three faulting types, but differ near the ends with the strike-slip data being lower than the reverse and normal faulting data. We also compare these U.S. models with a Japan model and data. The Japan model is also similar to the U.S. models near the center of the fault but decays less rapidly near the ends of the fault. In addition, we discuss impacts of models developed to analyze off-fault strain on secondary faults, multi-strand displacement hazard, and various mapping quality factors. We show example fault displacements for a M 7 fault with recurrence of 800 and 1600 years. We conclude that a deterministic assessment of fault displacements is often higher than the probabilistic displacements for less active faults with earthquake rupture recurrence that is longer than the hazard return period of interest. Choosing the appropriate hazard level is a challenging and important issue when applying PFDHA in engineering applications for buildings, bridges, pipelines, and nuclear facilities.

An important issue in PFDHA is uncertainty in where surface rupture would occur in future earthquakes. We illustrate methods to quantify two kinds of location uncertainties (epistemic uncertainty and aleatory variability). Epistemic uncertainty is associated with the mapping inaccuracy of existing fault traces. Aleatory variability is randomness in the exact location of future surface rupture around a previously existing, accurately located earthquake fault. We demonstrate a GIS-based approach for quantifying epistemic uncertainty using published Alquist-Priolo (AP) Earthquake Fault Zone maps as an example because AP maps are widely distributed and routinely referenced in engineering practice in California. Improved surface fault traces are obtained by careful interpretation of fault features using high-resolution LiDAR and other imagery. A statistically significant dataset is developed by systematically measuring the distances between improved and previously mapped traces. To quantify aleatory variability, we analyze paleoseismic trenches that reveal multiple events at the same site and re-analyze numerous trench logs from decades of fault investigations for research and development projects. Example fault displacement hazard maps are shown to demonstrate that estimated probabilistic fault displacement hazards can be better constrained and are likely reduced if uncertainty due to mapping inaccuracy can be removed or reduced and if aleatory variability in future surface rupture location can be quantified.

Risk Characterization and Dam Safety Modifications to Address Active Fault Rupture Beneath an Embankment Dam

David C. Serafini, P.E., G.E. Senior Geotechnical Engineer, US Army Corps of Engineers, SPD Dam Safety Production Center, 1325 J Street, Sacramento, CA 95814; david.c.serafini@usace.army.mil

Keith I. Kelson, C.E.G. Engineering Geologist, US Army Corps of Engineers, SPD Dam Safety Production Center, 1325 J Street, Sacramento, CA 95814; keith.i.kelson@usace.army.mil

Henri V. Mulder, P.E. Senior Geotechnical Engineer, US Army Corps of Engineers, Sacramento District, 1325 J Street, Sacramento, CA 95814; henri.v.mulder@usace.army.mil

Isabella Reservoir is located on the Kern River 34 miles upstream of the City of Bakersfield in Kern County, California. Isabella Dam has been designated as a Dam Safety Action Class (DSAC) I project by the U.S. Army Corps of Engineers (USACE), requiring action to reduce probabilities of failure and associated consequences. Isabella Dam construction began in 1948 and was completed in 1953, and consists of two embankment dams that provide flood control, water supply, power generation and recreation benefits to the region. The Main Dam is 185 feet high and 1,695 feet long, and the Auxiliary Dam is 100 feet high and 3,260 feet long.

This paper includes an overview of the dam safety project, and specifically a summary of the potential risk and dam safety modification design to address the potential for active fault rupture of the Kern Canyon fault beneath the right abutment of the Auxiliary Dam. Comprehensive geologic and paleoseismic investigations define a 150-foot-wide zone of active, east-down faulting in the right abutment of the dam, and show that the Kern Canyon fault has an average rupture recurrence of 3,200 years and average coseismic displacement of 3.6 feet. This paper discusses the amounts coseismic slip expected during large, surface-rupturing earthquakes, which were evaluated based on (1) site-specific paleoseismic data and worldwide empirical data on event-to-event slip variability, and (2) scenario-based fault displacements using empirical relationships between earthquake magnitude and surface displacement. The earthquake rupture scenarios developed from fault-specific paleoseismic and geologic analysis were used to interpret the expected range of earthquake magnitudes, the frequency of these earthquake magnitudes, and the annual exceedance probabilities of co-seismic displacement using probabilistic fault displacement hazard analytical methodology.

The results from the geologic and paleoseismic investigations and analyses helped to inform design of the size and location of filter and drain zones for the downstream buttress modification of the Auxiliary Dam. This paper also discusses the design approach to the thicknesses of the filter and drain layers, considering the possibility of coseismic transverse cracking and resultant internal erosion and piping of embankment material near the base of the dam. The mitigation measures are designed to reduce the probability of dam distress from coseismic rupture and propagation of transverse cracks in the base of the embankment, and therefore to mitigate the potential failure mode of breach related to fault rupture in the dam foundation.

50 or 500? Current Issues in Estimating Fault Rupture Length

David P. Schwartz
US Geological Survey
Menlo Park, CA

The potential rupture length of a fault is a primary input, and an uncertainty, for seismic source characterization. Rupture length is a critical parameter for estimating earthquake magnitude, whether used alone, in magnitude-area relations, or in moment magnitude calculations. Lacking site-specific fault displacement data across a design footprint, which is the case at most fault crossings, magnitude-displacement scaling relations can yield estimates of slip that can be manipulated for use in fault displacement hazard analyses.

Most faults of interest have not ruptured historically let alone repeatedly. Defining the future rupture length of an earthquake source has been a challenge since the beginning of source characterization in the 1970s, when simple concepts of full fault rupture and half fault rupture were employed. The question, of course, has always been what is a full fault rupture? The past several decades have seen source models developed in which faults have been divided into potential rupture segments that are defined on the basis of fault-specific behavioral data (rupture event timing, slip rate changes, transitions from locked to creep, microseismicity distribution) and kinematic variables (steps, branch points, bends, changes in trace complexity). These models, which are now being termed prescribed segmentation, have produced single and multi-segment ruptures for use in a broad range of earthquake probability and regional ground motion estimates. The most recent major study using this general approach is the 2016 source characterization of the Wasatch fault and associated normal faults of the Wasatch Front in Utah, Idaho, and Wyoming (WGUEP, 2016).

Alternatively, the 2013 Uniform California Earthquake Rupture Forecast (UCERF 3) (Field et al., 2014) opted to relax prescribed segmentation. This was guided by a set of rules in which a surface separation distance of ≤ 5 km and appropriate orientation to modeled Coulomb stress changes at fault junctions are the primary factors in permitting fault-to-fault jumps. A set of 350 fault sections produced 253,706K ruptures, the large majority of which involved multiple faults. Ruptures range in length from 15 km to 1200 km. 15% are ≤ 100 km, 45% are 100-500 km, and 40% are 500-1200 km. An inversion provides the rate of each rupture, which ranges from 10^2 - 10^8 years. Many have exceedingly low probabilities within the long-term UCERF 3 geologic model.

Worldwide, since 1850, ~ 280 surface ruptures in shallow continental crust (all tectonic settings and a broad range of slip rates) have been recognized. 71% are ≤ 49 km; 6% (only 17 events) exceed 150 km, and the longest is 1906 San Francisco (470 km). In California, since 1857, there have been 32 surface ruptures. The longest are 1906 San Francisco, 1857 Fort Tejon (350 km), and 1872 Owens Valley (108-120 km). 77% of California ruptures are shorter than 49 km in length. Most long (≥ 100 km) historical strike-slip ruptures have occurred as generally continuous, geomorphically well-defined (although not without localized complexity) traces with limited fault-to-fault jumps or branching, and they often represent only partial rupture of much longer and through going fault zones. In contrast, UCERF3 modeling of the southern Hayward fault (creeping), which ruptured in 1868, allows it to participate in ruptures that branch, jump, and extend to the south ends of the San Andreas and San Jacinto faults; these ruptures include propagation across the rapidly creeping sections of the Calaveras and San Andreas faults.

Modeling fault rupture length by relaxing segmentation, as exemplified by UCERF 3, does so without incorporating a range of physical factors that control what length a rupture might attain:

timing of the most recent prior earthquake(s) along strike (the 2002 Denali to Totschunda fault rupture propagation is an example of this); differences in strain accumulation on adjacent fault sections; paleo slip distributions; rupture dynamics including regional and local stress effects at branch points or steps; lithological and frictional variability; and the effects of creep, particularly on dynamic rupture propagation. Fault connectivity at depth, and not only a surface separation distance, is an important consideration. Combining these types of data and their interpretations (which can be difficult to obtain) with source-specific behavioral and kinematic observations can lead to effective construction of reasonable rupture models, including single-segment, multi-segment, and multi-fault scenarios for near-future earthquakes of interest. There is no reason why this cannot be prescribed by expert groups. For many faults under consideration for hazard analysis worldwide, this may be the most effective approach.

Field, E. H., G. P. Biasi, P. Bird, T. E. Dawson, K. R. Felzer, D. D. Jackson, K. M. Johnson, T. H. Jordan, C. Madden, A. J. Michael et al. (2014). Uniform California Earthquake Rupture Forecast, version 3 (UCERF3)—The time-independent model, *Bull. Seismol. Soc. Am.* 104, 1122–1180, doi: 10.1785/0120130164.

Working Group on Utah Earthquake Probabilities (WGUEP): Wong, I., W. Lund, C. DuRoss, P. Thomas, W. Arabasz, A. Crone, M. Hylland, N. Luco, S. Olig, J. Pechmann et al. (2016). Earthquake Probabilities for the Wasatch Front Region in Utah, Idaho, and Wyoming, *Utah Geol. Surv. Misc. Pub.*, 16-3, Utah Geological Survey, Salt Lake City, Utah.

Deterministic and probabilistic fault displacement hazard methodologies for gas pipeline crossings in California: applications and data needs

Thompson, Stephen^{1*}, Madugo, Chris², Lewandowski, Nora¹, Givler, Robert¹, Lee, Chih-Hung³, Ingermanson, Bronson⁴, and Hull, Alan⁵

¹Lettis Consultants International, Inc., Walnut Creek, CA

²Pacific Gas and Electric Company, Geosciences, San Francisco, CA

³Pacific Gas and Electric Company, Pipeline Engineering, San Ramon, CA

⁴Pacific Gas and Electric Company, Asset Integrity and Risk Management, San Ramon, CA

⁵Golder Associates, Inc., Redmond, WA

*thompson@lettisci.com

Abstract

Pacific Gas and Electric's extensive network of gas transmission pipelines overlaps California's extensive network of seismogenic faults. Understanding and mitigating the risk of pipeline failure from surface-fault rupture is a considerable engineering and seismological challenge to the utility. While the primary role and responsibility of the seismic and engineering geologists is to define the location and width of the fault crossing, and estimate the expected direction of fault displacement and/or folding at the pipeline, there is also the challenge of defining the deformation amount that should be considered by pipeline engineers to evaluate whether existing pipelines have adequate strain capacity to maintain pressure integrity should a displacement event occur. To this end, PG&E is implementing a fault displacement hazard analysis methodology to quantify displacement hazard at each pipeline-fault crossing.

In keeping with current engineering practice focused on deterministic evaluation, our approach is to develop displacement hazard estimates for "Maximum Considered Earthquake (MCE)" scenarios that produce surface-fault displacement at the pipeline. Rather than the traditional deterministic approach of adopting a single MCE magnitude and an MCE displacement from a simple empirical scaling relation (e.g., Honegger and Nyman, 2004), our methodology considers epistemic uncertainty in the MCE through logic trees, and epistemic and aleatory uncertainties in the amount of displacement that may occur at the pipeline crossing site given the MCE. MCEs themselves may be selected from community hazard models (e.g., WGCEP, 2003; Field et al., 2013) or may be constructed from analysis of "large but plausible" rupture lengths derived based on empirical constraints such as fault stepovers, gaps, and ends (e.g., Biasi et al., 2013; Biasi and Wesnousky, 2016). Alternative empirical relations between displacement and magnitude (Wells and Coppersmith, 1994) or displacement and length (Wesnousky, 2008; Shaw, 2013) may be selected, and epistemic uncertainty in how these relations should be centered is incorporated in the analysis.

The scenario displacement hazard is presented as an exceedance curve from zero to one and from which different statistical levels of displacement hazard may be tabulated. The pipeline engineers can then model pipeline response to specific displacements, with the statistical level of displacement specified based on a "consequence-hazard" matrix that considers both consequence of failure and fault activity (similar to Fraser and Howard, 2002). Displacement hazard information presented and analyzed in this way can readily be deconstructed to assess which parameters contribute most to hazard uncertainty. This "hazard sensitivity" information

can be used by the client to evaluate whether the collection of additional information is worthwhile.

The greatest opportunity to reduce displacement hazard uncertainty is through the collection and analysis of historical or paleoseismic data on surface displacements at or near the pipeline crossing of interest. The slip-at-a-point coefficient of variation information published by Hecker et al. (2013) and a methodology for deriving displacement hazard based on site-specific prior slips by Abrahamson (2008) result in much lower uncertainties in hazard over the process of exploring alternative MCE rupture scenarios and alternative empirical displacement relations.

The methodology can also incorporate information on fault slip rate or recurrence interval to convert deterministic exceedance curves into equivalent, simplified probabilistic hazard curves (Youngs et al., 2003). The intended use of the simplified probabilistic hazard curves for the PG&E gas pipeline network is as a ranking tool, whereby each pipeline-fault crossing can be “scored” or ordered by the annual probability of surface displacement exceeding the current pipeline capacity. We anticipate such information will be useful for prioritizing pipeline mitigation projects and will make the overall system more resilient to seismic hazards.

References

- Abrahamson, N., 2008. Appendix C—Probabilistic Fault Rupture Hazard Analysis, in San Francisco Public Utilities Commission (SFPUC), *Seismic Design Criteria*, revised 2008, 7 pages.
- Biasi, G.P. and Wesnousky, S.G., 2016. *Bulletin of the Seismological Society of America* **106** (3): 1110–1124.
- Field, E.H., and 17 others, 2013. *Uniform California Earthquake Rupture Forecast, Version 3 (UCERF3)—The Time-Independent Model*: U.S. Geological Survey Open-File Report 2013-1165.
- Fraser, W.A., and Howard, J.K., 2002. *Guidelines for use of the consequence-hazard matrix and selection of ground motion parameters*, The Resources Agency, Department of Water Resources, Division of Safety of Dams, 9 pages. Available online at: www.water.ca.gov/damsafety/docs/CHM.pdf, last accessed 5/29/2015.
- Hecker, S., Abrahamson, N.A., and Wooddell, K.E., 2013. Variability of displacement at a point: Implications for earthquake-size distribution and rupture hazard on faults, *Bulletin of the Seismological Society of America* **103** (2A): 651–674.
- Honegger, D.G. and Nyman, D.J., 2004, *Seismic Design and Assessment of Natural Gas and Liquid Hydrocarbon Pipelines*, Pipeline Research Council International, Inc., No. L51927.
- Shaw, B.E., 2013. Appendix E—Evaluation of Magnitude-Scaling Relationships and Depth of Rupture: in Field, E.H., Biasi, G.P., Bird, P., Dawson, T.E., Felzer, K.R., Jackson, D.D., Johnson, K.M., and 11 others [Working Group on California Earthquake Probabilities], 2013. *Uniform California Earthquake Rupture Forecast, Version 3 (UCERF3)—The Time-Independent Model*, U.S. Geological Survey Open-File Report 2013-1165, 23 pp.
- Wells, D.L., and K.J. Coppersmith, 1994. New empirical relationships among magnitude, rupture length, rupture width, rupture area, and surface displacement, *Bulletin of the Seismological Society of America*, **84**: 974-1002.

- Wesnousky, S.G., 2008. Displacement and geometrical characteristics of earthquake surface ruptures: Issues and implications for seismic hazard analysis and the earthquake rupture process, *Bulletin of the Seismological Society of America*, **98** (4): 1609-1632.
- Wesnousky, S.G., and Biasi, G.P, 2011. The length to which an earthquake will go to rupture, *Bulletin of the Seismological Society of America*, **101** (4): 1948–1950.
- Working Group on California Earthquake Probabilities, 2003. *Earthquake probabilities in the San Francisco Bay region; 2002–2031*: U.S. Geological Survey Open-File Report 2003-214.

Widespread complex surface rupture associated the Mw 7.0 16 April 2016 Kumamoto, Japan, earthquake

Shinji Toda¹ Yasuhiro Kumahara², Hideaki Goto², and Research Group for Surface Rupture of the Kumamoto Earthquake

¹International Research Institute of Disaster Science (IRIDeS), Tohoku University, Japan, toda@irides.tohoku.ac.jp

²Hiroshima University, Japan.

The 16 April 2016 Mw=7.0 (Mjma=7.3) Kumamoto earthquake struck the city of Kumamoto, towns of Mashiki, Nishihara and Minami-Aso in central Kyushu, southwest Japan, and brought significant damage to buildings, killing 50 people. An ENE-trending ~31-km-long surface rupture emerged during the earthquake along the previously mapped Futagawa and northern Hinagu faults. The rupture zone also included a previously unknown 5-km-long fault within the Aso Caldera, one of the active volcanos in Kyushu island. The hypocenter is located ~5 km west from the junction of the Futagawa and Hinagu faults those strikes compose of a 25°-transpressional bend. The 14 April 2016 Mw=6.2 (Mjma=6.5) earthquake, claimed as a foreshock, was preceded on the Hinagu fault zone, 2.5 km south of the fault junction. From the viewpoints of fault displacement hazard assessment, we here present three key features as a lesson learnt from the Kumamoto earthquake.

1) Unpredictable multiple scale en echelon step-overs and short conjugate faults

The rupture zone is mostly composed of right-lateral slip sections, with a maximum of 2.5 m coseismic slip. On a scale of 1:50,000 map, most of the rupture traces preoccupied the previously mapped faults that already display fault branching and multiple parallel traces, except the ones inside the Aso Caldera. However, observed surface breaks are much more complex than the inferred ones in large scale maps. A remarkable feature was left-stepping en echelon step-overs on various scales from meters to a few kilometers. The other significant characteristic is several short NW-trending left-lateral faults (up to ~300 m) as a conjugate fault to the primary right-lateral fault. These unpredictable features are probably due to the combination of thick unconsolidated volcanic sediments derived from the caldera and complex structure in and around the fault junction.

2) Coseismic slip partitioning

Another noteworthy feature observed in the field are ~10-km-long segmented normal fault scarps, dipping to the north-west, mostly along the previously mapped Idenokuchi fault, 1.2 to 2.0 km south of and subparallel to the Futagawa fault. The maximum amount of coseismic throw on the Idenokuchi fault is ~2 m, which is nearly equivalent to the maximum slip on the strike-slip rupture. The locations and slip motions of the 2016 rupture also manifest as interferogram fringe offsets in InSAR images. Together with geodetic and seismic inversions of subsurface fault slip, we illustrate a schematic structural model where oblique motion occurred on a north-west-dipping subsurface fault and the slip is partitioned at the surface into strike-slip and normal fault scarps. The Kumamoto case would be the second significant slip-partitioned earthquake around the globe.

3) Triggered slips on short peripheral faults

Multiple InSAR images for the Kumamoto earthquake consistently display more than 200 triggered fault slips as offsets of interferogram fringes around the primary rupture zone (e.g.,

Fujiwara et al. 2016, Earth Planets, and Space). While slips on most of them are smaller than a range of one interferogram fringe (~12 cm), significant multiple slips larger than 20 cm occurred in a part of the mountainous outer rim of the Aso caldera, ~15 km far away from the main rupture zone, without any significant aftershocks. We found a ~6-km-long NW-trending discontinuous minor breaks bisecting the urbanized area of Kumamoto, which might have been related to local damage. The post-earthquake geomorphic investigation using vertically exaggerated anaglyph images suggests these fractures occurred on the pre-existing faint normal fault scarps.

Application or Mis-Application of PFDHA. What Relationships are Appropriate and Is the Displacement Result Reasonable?

Donald Wells
Amec Foster Wheeler

Probabilistic fault displacement hazard analysis (PFDHA) is a relatively new tool for assessing design displacements for projects such as buildings, bridges, tunnels, pipelines, dams, and other infrastructure and transportation facilities that cross or lie astride active faults. While the basic methodology for PFDHA has been understood for nearly 20 years, and a detailed description of PFDHA methodology and relationships for normal faulting were published in 2003, empirical relationships describing slip distributions for strike slip and reverse faulting were not published until 2011. While that availability of slip distributions for all three types of faulting significantly improves the applicability of PFDHA for different tectonic environments, the available models, empirical relationships, and details of the methodology require numerous explicit choices by the practitioner to perform PFDHA. Thus, the state of practice in performing PFDHA appears to vary widely, and the results of individual studies appear to vary widely as well, depending on how the PFDHA is implemented.

This study addresses several aspects of the PFDHA process through sensitivity analyses, with a goal of providing information to improve and standardize the practice of PFDHA. For the analyses presented in this study, we assume that the project facility overlies an active fault trace, and we assess fault rupture hazard from primary faulting without considering uncertainty in fault location.

Given a fault, with assessment for fault length, rupture length, and slip rate, the PFDHA then includes assessment for:

- Probability of Surface Rupture (PSR);
- Probability of Rupture Reaching Site; and
- Expected Displacement Given Location of Site Along a Rupture

The sensitivity analyses presented in this study address approaches to assess the probability of surface rupture, and the effects of fault source characterization, specifically the effect of site location with respect to location along ruptures, for the assessment of the probability of ruptures reaching the site and the expected displacement at the site.

Probability of Surface Rupture (PSR)

The probability of surface rupture (PSR) typically is assessed using an empirical relationship that expresses the probability of surface rupture as a function of magnitude. The functional form of this relationship typically is a logistic regression, and regression relationship may be based on global or regional databases of earthquakes with and without surface ruptures. The databases also may be parsed by fault type. However, the resulting PSR does not account for the expected focal depth of the earthquake or the rupture width.

An alternative approach, termed the “geometry approach” is based on the expected fault width and the observed depth distribution of earthquakes along the fault or surrounding region. For the geometry approach, the expected rupture width is calculated for each magnitude based on the scenario rupture length and an assigned rupture aspect ratio for the expected fault type. The maximum depth of rupture is distributed following the focal depth distribution of local or regional

earthquakes, and the PSR at each magnitude is the percentage of ruptures that extend to the surface given the rupture width and maximum depth distribution. This approach requires more information to implement, but is appropriate if detailed information on the depth distribution of earthquakes is available. The fault geometry approach is sensitive both to the aspect ratio, which may be about 1:1 for reverse and normal faulting, and about 2:1 or larger for strike-slip faulting, and to the maximum depth distribution for the fault. Specifically, the geometry approach has an increasing effect (reducing the PSR) with increasing depth of rupture compared to the regression approach, particularly for ruptures with small aspect ratios.

Effects of Fault Source Characterization

The available models for slip variability along a rupture all show significantly reduced displacement near the end of a rupture. Therefore, little displacement occurs for any rupture scenario where the site is located close to the end of the rupture. If the fault source model is based on fault segments with fixed endpoints and a limited number of rupture scenarios such as presented in UCERF2 (USGS Open File Report 2007-1437), and the site is located near the end of a fault segment, the resulting displacement hazard will be low compared to that for a site located in the middle of the fault segment. However, many historical earthquakes have ruptured across multiple faults, indicating that the ends of many of the fixed faults in the UCERF2 model may not always represent the end of ruptures. Thus, a fault source model with a broad range of multi-fault ruptures and a range of locations for endpoints for fault ruptures, such as presented in UCERF3 (USGS Open File Report 2013-1165), likely will result a higher displacement hazard for many sites compared to a fixed fault segment model, if ruptures extend to a nearby fault such the site is not always located at the end of the rupture. This observation indicates that the choice for location of fault ruptures, where they start and stop, as well as choices for the length of ruptures have a strong influence on the displacement hazard.

Another effect of limited fixed fault and rupture segments in the UCERF2 fault characterization is that the displacement hazard may be higher for short ruptures compared to long ruptures, because less time is required to accumulate sufficient strain corresponding to the expected displacement for moderate magnitude earthquakes compared to the time required to accumulate the strain associated with larger displacements expected for larger magnitude earthquakes. The specific effect on displacement hazard is dependent on the difference in length/area of the ruptures as related to expected displacement, the PSR, the percentage of ruptures that reach the site, and the site location along the fault. The tradeoffs between fault slip rate, rupture length/area, magnitude, and recurrence are important to displacement hazard, particularly for low slip-rate faults. Specifically, for longer ruptures with higher magnitudes, if the recurrence period (from the magnitude and slip rate) is longer than the time period of concern for performance analysis, the displacement hazard is zero for that rupture scenario (i.e., the hazard curve lies below the design level frequency of exceedance of displacement). Conversely, for shorter ruptures with lower magnitudes, while the recurrence period may be shorter than the time period of concern for performance analysis (and the hazard curve extends above the design level frequency of exceedance), the expected displacement will be small compared to that for a larger magnitude earthquake.

Another consideration is the use of alternative rupture lengths for a given fault scenario. While alternative rupture lengths that are shorter than the total fault length would be associated with a shorter average recurrence interval, because the rupture location is randomized along the fault,

not all of the shorter ruptures will extend to the site, and the hazard is factored for the percentage of ruptures that do not cross the site.

Summary Considerations

The sensitivity of tradeoffs among alternative models, input parameters, site location, and expected displacement show that the displacement hazard can vary widely depending on the choices made in assessing fault characteristics and performing the PFDHA. To minimize subjectiveness in evaluating displacement hazard, these choices should be informed by as much knowledge of the site setting and fault characteristics as possible. Specific considerations and data that can help inform choices to prepare the displacement evaluation include paleoseismic data, geomorphic expression of faulting, structural complexity of faulting, and potential for continuity of rupture to nearby faults. In addition, assessments that may be performed to interpret/disaggregate the displacement hazard results include calculating the effective fault slip rate from the hazard curve for consistency with the slip rate used in the source model, evaluating the magnitude contributions to hazard, and evaluating the magnitude frequency distribution for comparison to the preferred distribution model (i.e., characteristic earthquake or other models). This additional information provides a basis for assessing whether those small displacement estimates (or other results) are reasonable and appropriate.

U.S. Criteria for Assessing Tectonic Surface Fault Rupture and Deformation at Nuclear Facilities

ANSI/ANS-2.30 Working Group

Ivan Wong, *Lettis Consultants International, Walnut Creek, CA*

Bill Bryant, *California Geological Survey, Sacramento, CA*

Rui Chen, *California Geological Survey, Sacramento, CA*

Keith Kelson, *U.S. Army Corps of Engineers, Sacramento, CA*

Jeff Kimball, *Rizzo Associates, Pittsburg, PA*

Joe Litehiser, *Bechtel Corporation, San Francisco, CA*

Susan Olig, *Olig Seismic Geology, Pleasant Hill, CA*

David Schwartz, *U.S. Geological Survey, Menlo Park, CA*

Alice Stieve, *U.S. Nuclear Regulatory Commission, Rockville, MD*, and

Donald Wells, *AMEC Environment & Infrastructure, Oakland, CA*

ANSI/ANS-2.30 "Criteria for Assessing Tectonic Surface Fault Rupture and Deformation at Nuclear Facilities" is a standard that provides criteria and guidelines for assessing permanent ground deformation (PGD) hazard due to tectonic surface fault rupture and deformation at nuclear facilities. Specifically, the purpose of the standard is to provide an outline of procedures and methods for performing probabilistic fault displacement hazard analysis (PFDHA) and probabilistic tectonic deformation hazard analysis (PTDHA). The hazard assessment may focus on displacement of a principal fault or on distributed faulting related to the principal fault.

The standard also provides guidance on site selection for Seismic Design Category (SDC)-3 to SDC-5 nuclear facilities. The results of the hazard assessment can be used in siting of a nuclear facility and as a basis for a decision regarding whether the site is acceptable for design and operation.

ANSI/ANS-2.30 is one of a series of national standards designed to provide criteria and guidelines to promote uniform and effective assessment of seismic hazards at nuclear facilities. These hazards must be properly identified and characterized commensurate with the level of risk and design-requirements associated with each nuclear facility.

Issues associated with setback distance from active faults in China: What we have learned from the 2008 Wenchuan Earthquake

Xiwei Xu¹, Tingting Guo², Shaozhuo Liu¹, Guihua Yu¹, Guihua Chen¹, Xiyun Wu¹

¹Institute of Geology, China earthquake Administration, Beijing 100029

²Earthquake Administration of Shandong Province, Jinan 250014

Living with disaster is an objective reality that human must face, especially in China. A large number of recent earthquakes, such as the 2008 Wenchuan earthquake, 2010 Yushu earthquake, 2014 Ludian earthquake, have demonstrated that earthquake heavy damages and casualties stem mainly from ground-faulting or displacement along a seismogenic active fault and near-fault ground accelerations. Accordingly, avoidance of active faults may be an important measure effectively to reduce earthquake hazard, which may encounter in the future, but how to avoid an active fault and how much a setback distance from the active fault is required to ensure that the ground faulting and displacement has no any direct impact on buildings. This has been focus of debate both for domestic and foreign scholars in the past years.

Studies have shown that almost all different types of earthquake surface rupture zones are characterized by high localization along their seismogenic active faults both from field observations and paleoseismic trenches (Lee et al., 2001 ; Kelson & Lettis, 2000 ; Bray, 2001 ; Yang & Beeson, 2001 ; Rockwell & Ben-Zion, 2007 ; Xu et al., 2002, 2009 ; Zhou et al., 2010; Quigley et al., 2010). An average statistic width is obtained to be 30m for the known strike-slip faulting earthquakes surface rupture zones (Xu et al., 2002), which has been supported by late observations in the 2001 Kokoxili, 2002 Denali, 2010 Yushu, 2014 Ludian earthquake (Xu et al., 2002, 2015; Eberhart-Phillips et al., 2003; Sun et al., 2012). The surface ruptures in the reverse-faulting events, such as the 1999 Chi-Chi or the Wenchuan earthquake, also display a high degree of localization in width, but demonstrate a more complicated rupturing pattern (Chen et al., 2001; Xu et al., 2009), which gives us a chance to consider reducing related earthquake hazards. Quantitative analyses show that the surface ruptures of the Wenchuan earthquake have following features:

- 1) The width-frequency distribution of the surface rupture zones of the Wenchuan earthquake measured at different sites indicate a mean value (μ) of (22.4 ± 1.8) m and a mean square error (σ) of (12.3 ± 1.3) . If $\mu + 2\sigma$ is used as an average width, then we know that the average width, which may occur in a reverse-faulting faulting earthquake, is 49 ± 2 m with a confidence more than 95%.
- 2) The surface ruptures of the reverse-faulting earthquakes shows an asymmetrical distribution along the reverse fault. Width of surface ruptures on the hanging-wall is 2 or 3 times wider than that on its foot-wall for a reverse fault, demonstrating a hanging-wall effect for a reverse fault.
- 3) Correspondingly, the co-seismic displacements along seismogenic fault directly controls spatial distribution of the ground building damages with a similar pattern to the surface ruptures along the fault, which also demonstrates a hanging-wall effect.
- 4) Based on the latest knowledge learnt above, issues on avoidance object, minimum setback distance, location requirement of active fault for avoidance, and anti-faulting design for buildings in the surface rupture zone should be further discussed.